Doctoral Thesis

Involvement of TRPV2 in the differentiation of mouse brown adipocytes

Wuping SUN

Division of Cell Signaling

Okazaki Institute for Integrative Bioscience

(National Institute for Physiological Sciences)

Department of Physiological Science

School of Life Science

The Graduate University for Advanced Studies (SOKENDAI)

2014

Summary

The prevalence of obesity has increased in worldwide, and obesity is believed to be a result from an imbalance between intake of energy and energy expenditure. Obesity is characterized by increased adipose tissue mass that results from increased fat cell size and number. It is well known that there are two types of adipose tissue, a white adipose tissue (WAT) and a brown adipose tissue (BAT). Importantly, it has been reported that BAT also exists in adult humans. Therefore, understanding the molecular mechanisms for differentiation of not only white adipocytes, but also brown adipocytes has been the subject of intense investigation. It has been reported that the increase in intracellular calcium levels in 3T3-L1 pre-adipocytes by calcium-mobilizing reagents including ionomycin or a calcium-ATPase inhibitor, tharpsigargin (TG) efficiently inhibits differentiation, diminishes adipocyte-specific gene expression and reduces lipid accumulation. However, the effect of $[Ca^{2+}]_i$ increase on brown adipocyte differentiation is still not known.

Most of transient receptor potential (TRP) ion channels are non-selective calcium permeable cation channels that were originally discovered in mutant Drosophila that responded abnormally to a light stimulus. Among these members of the TRP channels, TRPV2 also functions as a non-selective calcium-permeable cation channel and is composed of six trans-membrane domains with a putative pore-loop region. TRPV2 is activated by noxious heat, with an activation temperature threshold of higher than 52 °C, and by a number of exogenous chemical ligands, e.g. 2-aminoethoxydiphenyl borate (2APB) and lysophosphatidyl choline (LPC), with a species specific manner. SKF96365 (SKF) is a TRPV2-selective antagonist. Importantly, TRPV2 is also reported as a mechano-sensitive channel activated by

mechanical stretch and cell swelling. However, the expression and physiological role of TRPV2 in brown adipocytes are still unknown.

Therefore, I hypothesized that TRPV2 is functionally expressed in brown adipocytes and that TRPV2 activation induces calcium influx, which could regulate brown adipocyte differentiation. My aim is to investigate the involvement of TRPV2 in mouse brown adipocytes differentiation.

This study was conducted and investigated from different levels, from molecular identity to channel function. *Trpv2* mRNA and TRPV2 protein expression levels were analyzed in primary cultured mouse brown adipocytes using RT-PCR and Western blotting methods, and functional expression level of TRPV2 was examined using calcium-imaging and whole-cell patch-clamp methods. Pharmacological studies were conducted with TRPV2 agonists, 2APB and LPC, and a selective antagonist SKF. Mechanical stimulation was applied using a 3-D sunflower mini shaker in the CO_2 incubator. Brown adipocytes differentiation was assessed by counting differentiated brown adipocyte numbers and measuring triglyceride levels.

Trpv2 was dominantly expressed in brown adipocytes among *Trpv1*, *Trpv2*, *Trpv3* and *Trpv4*, and TRPV2 was also functionally expressed in brown adipocytes. Functional expression of TRPV2 was dramatically increased during the differentiation of mouse brown adipocytes. Moreover, pharmacological studies demonstrated that activation of TRPV2 prevents the differentiation of mouse brown adipocytes via a calcineurin-dependent pathway. Mechanical stimulation inhibited mouse brown adipocyte differentiation via TRPV2 activation. Differentiated adipocyte numbers and triglyceride levels in the isolated brown adipocytes from

interscapular BAT (iBAT) were not different between WT and TRPV2-knockout (TRPV2KO) mice in the 6 day-differentiation. However, TRPV2 agonists and mechanical stimulation inhibited brown adipocyte differentiation more effectively in WT than in TRPV2KO adipocytes. FK506 and cyclosporine A rescued TRPV2 activation-induced inhibition of mouse brown adipocyte differentiation, suggesting that TRPV2 activation-induced inhibition of mouse brown adipocyte differentiation occurred via a calcineurin-dependent pathway. iBAT weights per body weights were significantly larger in TRPV2KO than in WT mice. And TRPV2KO mice showed increased brown adipocyte cell sizes and impaired thermogenesis in response to β_3-agonist application.

In conclusion, TRPV2 is functionally expressed in mouse brown adipocytes and plays an important role in regulating mouse brown adipocyte differentiation. Membrane stretch possibly due to the increase in brown adipocyte volume through lipid droplet accumulation induced activation of TRPV2, which might prevent mouse brown adipocyte differentiation via a calcineurin-dependent pathway. The fact that TRPV2 acts as a negative modulator in brown adipocyte differentiation suggests that TRPV2 might be involved in the prevention of iBAT over-growth. Therefore, TRPV2 would be a promising therapy target for human obesity treatment and prevention.

Table of contents

1. Introduction

The prevalence of obesity has increased in worldwide, and obesity is believed to be a result from an imbalance between intake of energy and energy expenditure [Ahn J et al., 2008]. Obesity is also a serious health problem that is implicated in various diseases including type II diabetes, hypertension, coronary heart diseases, and cancer [Pi-Sunyer FX., 2002]. Obesity is characterized by increased adipose tissue mass that results from increased fat cell size and number, suggesting that the main contributor to obesity is an adipose tissue [Hajer GR et al., 2008]. It is well known that there are two types of adipose tissues, a white adipose tissue (WAT) and a brown adipose tissue (BAT). However, the functions of these two types of adipose tissues are almost opposite [Lowell BB et al., 1997; Cannon B et al., 2004]. Compared with WAT, the main function of BAT is energy dissipation, or generating heat. BAT is a major site for mammalian non-shivering thermogenesis through mitochondrial uncoupling protein 1 (UCP1) [Argyropoulos G et al., 1985; Mozo J et al., 2005]. Most importantly, it has been reported that BAT also exists in adult humans as demonstrated using a combination of high resolution imaging techniques [Cypess AM et al., 2009; Van Marken Lichtenbelt, W.D. et al., 2009]. Thus, BAT could be a promising target for human obesity prevention and treatment. Therefore, understanding the molecular mechanisms for differentiation of not only white adipocytes, but also brown adipocytes has been the subject of intense investigation.

It is well known that calcium signaling is important for survivor and function maintenance of many cell types [A Ghosh and ME Greenberg, 1995; Michael J et al., 2003]. It has been reported that the increase in intracellular calcium levels in 3T3-L1 pre-adipocytes by calcium-mobilizing reagents including ionomycin or a calcium-

ATPase inhibibitor, tharpsigargin (TG) efficiently inhibits differentiation, diminishes adipocyte-specific gene expression and reduces lipid accumulation [Ntambi JM and Takova T, 1996; Shi H, et al., 2000]. These inhibitory effects were mimicked either by enhancing the activity of the Ca^{2+}/calmodulin-dependent serine/threonine phosphatase, calcineurin [Neal JW and Clipstone NA, 2002] or by constitutive activation of calcineurin effectors such as members of the nuclear factor of activated T cell (NFAT) family [Neal JW and Clipstone NA, 2003]. Conversely, inhibition of calcineurin activity by cyclosporin A (CsA) increased adipocyte differentiation and lipid accumulation [Neal JW and Clipstone NA, 2002], mimicking the obesogenic effects of CsA treatment in humans [Mathieu et al., 1994]. Importantly, CsA recovered the ionomycin-induced inhibition of 3T3-L1 adipocyte differentiation by inhibiting calcineurin activity [Neal JW and Clipstone NA, 2002]. These reports demonstrate that elevation of $[Ca^{2+}]_i$ has negative effects on white adipocyte differentiation similar to that seen in other cell types [Berridge MJ., 2006]. A previous report showed that increased calcium influx via a store operated calcium channel, Orai1, upon activation of an ER membrane protein, stromal interaction molecule-1 (Stim1), inhibited the differentiation of 3T3-L1 white adipocytes [Graham SJ et al., 2009]. However, the effect of $[Ca^{2+}]_i$ increase on brown adipocyte differentiation is still not known.

Transient receptor potential (TRP) ion channels are non-selective calcium-permeable cation channels that were originally discovered in mutant *Drosophila* that abnormally responded to a light stimulus [Montell C et al., 1989]. TRP channels have six trans-membrane (TM) domains (TM1 to TM6) and a pore loop between TM5 and TM6 with both N- and C-termini in the cytosol [Shigematsu H et al., 2010;

Moiseenkova-Bell VY et al., 2008]. TRP channels are unique cellular sensors characterized by a promiscuous activation mechanisms, such as thermo-sensor and mechano-sensor [Nilius B et al., 2007]. It has been reported that TRP superfamily of ion channels are widely expressed and play multiple functions [Caterina MJ et al., 1997; Tominaga M et al., 1998; Link TM et al., 2010; Uchida K., 2011]. The TRP channel superfamily is now classified into seven subfamilies: TRPV (Vanilloid), TRPC (Canonical), TRPM (Melastatin), TRPML (Mucolipin), TRPN (NomPC), TRPP (Polycystic) and TRPA (Ankyrin) according to their primary amino acid sequences rather than selectivity or ligand affinity because their properties are heterogenous and their regulation mechanisms are complicated.

Among these members of TRP channels, TRPV2 also functions as a non-selective calcium-permeable cation channel and is composed of six trans-membrane domains with a putative pore-loop region [Perálvarez-Marín, A., 2013; Caterina, MJ et al., 1999]. TRPV2 is activated by noxious heat with an activation temperature threshold of higher than 52 °C [Caterina, MJ et al., 1999] and by a number of chemical ligands, e.g. 2-aminoethoxydiphenyl borate (2APB) and lysophosphatidyl choline (LPC) with a species specific manner [Juvin V et al., 2007; Monet M et al., 2009]. SKF96365 (SKF) is a TRPV2-selective antagonist [Juvin V et al., 2007; Ramsey IS et al., 2006]. Importantly, TRPV2 is also reported as a mechano-sensitive channel activated by mechanical stretch and cell swelling [Muraki K et al., 2003; Iwata Y et al., 2009].

Since the expression and physiological role of TRPV2 in brown adipocytes are still unknown, I hypothesized that TRPV2 is functionally expressed in brown adipocytes and that TRPV2 activation induces calcium influx which could regulate brown adipocyte differentiation. In this study, I found that membrane stretch

possibly due to the increased cell volume of brown adipocytes upon lipid droplet accumulation induces TRPV2 activation which in turn inhibits brown adipocyte differentiation via a calcineurin-dependent pathway in mice. I also found that adipocytes in interscapular brown adipose tissue (iBAT) of TRPV2 null mice show increased cell sizes and that a β3-adrenergic receptor agonist, BRL37344-induced non-shivering thermogenesis was impaired in TRPV2-deficient (TRPV2KO) mice. These data suggest that TRPV2 is a negative modulator of brown adipocyte differentiation and that TRPV2 might be involved in the prevention of iBAT over-growth.

2. Materials and Methods

Animals

Male C57Bl/6NCr mice (SLC, Hamamatsu, Japan) were housed in a controlled environment (12 h light/dark cycle; 22-24°C; 50 - 60% humidity) with food and water *ad libitum*. All animal protocols were approved by the Animal Research Committee, National Institute for Physiological Sciences of Japan (NIPS, Okazaki, Japan).

TRPV2KO mouse generation

Generation of TRPV2KO mice is described elsewhere DNA encoding TRPV2 axon 3 to 5 was deleted, ablating channel function and detectable protein. To overcome prenatal lethality observed in TRPV2KO mice on C57Bl/6NCr background, we generated wild-type and $TRPV2^{+/-}$ F3 hybrids by crossing C57Bl/6NCr $TRPV2^{+/-}$ mice with ICR wild-type mice, and then $TRPV2^{+/-}$ F3 hybrids were mated to each other to generate F3 hybrids TRPV2KO mice. The resulting TRPV2KO mice appear healthy as wild type mice. The same background wild type (WT) mice were also obtained from crossing between $TRPV2^{+/-}$ F3 hybrids. Polymerase chain reaction (PCR) primers for genotyping were forward primer 5'-GTCTCACTGAACTCTGCTAGACTGG-3', reverse primer 1 5'-ATAGCCTGGGATACTCTGTCTCAAG -3', and reverse primer 2 5'-GTGATAACCACAGCAGAACATAGTG -3', yielding PCR products of 248 bp (WT allele) and 432 bp (null allele).

Primary culture of mouse brown adipocytes

The primary culture was followed by a previous method with slight modification [Irie Y et al., 1999]. In briefly, six mice (3-week old, male) were euthanized by dislocating the spine and interscapular BAT was isolated. And then collected iBAT tissues were minced and digested in 20 ml Dulbecco's modified Eagle's medium (DMEM) containing 2 mg/ml collagenase (Type 1, Sigma, St. Louis, MN, USA) and 2 % bovine serum albumin at 37°C for 45 min in a shaking machine at 85 strokes/min. The digest was filtered through a nylon screen (pore size 250 μm) and centrifuged at 1500 rpm for 2 min. The sediments were suspended and filtrated again through a nylon screen (pore size 60 μm). Resulting stromal vascular cells were seeded into two 60 mm culture dishes (Falcon, Austin, TX, USA) at a density of 20,000/cm^2 in DMEM supplemented with 10 % fetal calf serum (FCS, Gibco, Carlsbad, CA, USA), 100 units/mL penicillin and 100 units/mL streptomycin (Invitrogen, Carlsbad, CA, USA). After incubation at 37°C for 24 hr in an atmosphere of 5% CO_2 in air, attached cells were washed with PBS and incubated in the same medium with changing the medium every 2 days. After becoming confluent, the cells were inducted in standard medium supplemented with 3-isobutyl-1-methylxanthine (IBMX) 500 μM and dexamethasone (Dex) 1 μM (induction medium) at the standard incubation condition for 2 days, and then cells were differentiated in standard medium supplemented with 50 nM T3 and 100 mg/mL insulin (differentiation medium) for more 6 days. For all the pharmacological study, compounds were applied when medium was changed from the induction medium to the differentiation medium for 6 or 9 consecutive days to induce differentiation.

Cells were visualized using a light microscope at 10× magnification, and representative images were captured.

RT-PCR

Total RNA was isolated using Sepasol-RNA I Super G (Nacalai Tesque Inc., Kyoto, Japan) according to the manufacturer's protocol. In brief, mouse tissues or cells were freshly collected and homogenized in Sepasol-RNA I Super G on ice. Reverse transcription-PCR (RT-PCR) was performed using the SuperScript® III kit (Invitrogen) with the following conditions: 65 °C for 5 min, 50 °C for 50 min and 85 °C for 5 min. The RNA was digested with RNase H at 37 °C for 20 min. PCR was performed as follows: one cycle at 98 °C for 2 min; 35 cycles at 98 °C for 10 sec, 60 °C for 35 sec; 72 °C for 1 min. The primer sequence information was summarized in Table 1. The PCR products were separated on a 2% agarose gel in Tris–acetate EDTA buffer supplied with ethidium bromide and photographed using the UVP BIoDoc-It Imaging system (ATTO, Tokyo, Japan).

Real-time RT-PCR

Mouse *Trpv1, Trpv2, Trpv3* and *Trpv4* mRNA copy numbers were determined by qRT-PCR using SYBR Green (Invitrogen). The sequences of the forward and reverse primers were listed in Table 1. The qRT-PCR reaction volume contained 2 μL cDNA (1 μg/μL), 10 μL 2X Mastermix, 0.4 μL forward primer, 0.4 μL reverse primer and was brought to a final volume of 20 μL with nuclease-free water. Real-time RT-PCR cycling conditions were: one cycle at 95 °C for 10 min, 40 cycles at

95 °C for 15 sec, and 57 °C for 1 min, one cycle at 95 °C for 15 sec, one cycle at 55 °C for 1 min, and one cycle at 95 °C for 15 sec. Data were collected during each extension phase of the PCR reaction and analyzed using ABI-7700 SDS software (Applied Biosystems, Foster City, CA, USA).

Immunoprecipitation and Western blotting

HEK293T cells (5 x 10^5) were cultured on ten cm diameter petri dishes and allowed to grow overnight. Cells were transfected with *Trpv2* plasmids, which was a gift from Dr. Cepko C (Harvard University, Cambridge, MD, USA) using Lipofectamine reagent (Invitrogen) following the manufacturer's protocol as a positive control. Different differentiation stages of brown adipocytes from WT and TRPV2KO mice were collected by trypsin digestion at 37 °C for 5 min, and then centrifuged at 12,000 rpm (12,397 g) at 4 °C for 5 min and lysed in 100 μL RIPA lysis buffer with complete protease inhibitor cocktail (Roche Molecular Biochemicals, Basel, Switzerland). The nuclear and insoluble components were discarded following centrifugation at 12,000 rpm (12,397 g) at 4 °C for 5 min. The cell lysates were pre-cleared with protein G Sepharose beads (GE Healthcare, Little Chalfont, Buckinghamshire, United Kingdom) with rotation at 4 °C for 2 hr. The supernatants were collected after centrifugation at 1,000 rpm (1033 g) at 4 °C for 5 min and incubated with 2 μL anti-TRPV2 antibody (TransGenic, Kobe, Japan) at 4 °C overnight. The samples were precipitated with 20 μL protein G Sepharose beads (GE Healthcare) for 2 h in Micro Bio-Spin Chromatography Columns (Bio-Rad, Munich, Germany). The samples were washed three times with RIPA lysis buffer, and denaturized by adding 4x SDS buffer and 2 M DTT, heat shock at 95 °C for 5

min. The denaturized samples were separated on a 8% SDS-PAGE gel and transferred onto a PVDF membrane. The membrane was blocked using BlockAce reagent (Snow Brand Milk Products Co.) at 4 °C overnight and then incubated with an anti-TRPV2 antibody diluted 1:1000 at room temperature for 1 h. After three washes with PBS-T (0.1% Triton X-100), the membrane was incubated at room temperature for 1 h with an anti-rabbit IgG HRP-linked antibody (Cell Signaling Technology, Boston, MA, USA) diluted 1:5000. The signals were visualized with ECL kit (Pierce, IL, USA) and the PVDF membrane was photographed using a LAS-3000 imaging system (FUJIFILM, Tokyo, Japan).

Electrophysiology

For whole-cell patch-clamp recording experiments, mouse brown pre-adipocytes, 2 day- and 6 day- differentiated adipocytes were used. The standard bath solution contained 140 mM NaCl, 5 mM KCl, 2 mM $MgCl_2$, 2 mM $CaCl_2$, 10 mM HEPES and 10 mM glucose, pH 7.4, adjusted with NaOH. The pipette solution contained 140 mM KCl, 5 mM EGTA and 10 mM HEPES, pH 7.4, adjusted with KOH. Data were sampled at 10 kHz and filtered at 5 kHz using an Axopatch 200B amplifier (Axon Instruments, Sunnyvale, CA, USA). The membrane potential was clamped at -60 mV during the whole-cell patch-clamp recordings and a voltage-ramp from -100 mV to +100 mV for 300 ms was applied in a five sec period. All patch-clamp experiments were performed at 25 °C. Chemicals were applied for 30 sec to one min until a clear desensitization was observed. Data were analyzed using pCLAMP10.4 software (Axon Instruments).

Calcium imaging

Intracellular calcium concentration was monitored by loading primary cultured brown adipocytes with Fura-2 AM fluorescent dye (Invitrogen). Adipocytes were incubated with 1 μL Fura-2 AM for 30 min and used in experiments within 3 hr. Fluorescent signals were recorded by IP Lab software (Scanalytics, Inc., Rockville, MD, USA) at three sec intervals. The standard bath solution was the same as that used for whole-cell patch-clamp recordings. A positive response was obtained when the 340/380 ratio increased more than 0.2 evoked by 2APB or LPC. Norepinephrine (NE) responses indicated cells are differentiated brown adipocytes. Cell viability was confirmed with 5 μM ionomycin. All the experiments were performed at 25 °C.

Oil red O Staining of brown adipocytes

Mouse brown adipocytes were cultured in differentiation medium as described in brown adipocyte primary culture protocol. Oil red O staining was performed using oil red O dye (Sigma). In brief, the adipocyte culture dish was taken out of the incubator, the medium was removed, and then the cells were washed with PBS twice. The cells were fixed with 4% formalin and incubate at room temperature for at least 1 hr. After fixation, cells were washed with purified water (MilliQ) twice and washed with 60% isopropanol at RT for 5 min. The cells were let dried completely at RT, and oil red O solution was added and then incubated at RT for 10 min. Oil red O solution was removed with addition of purified water (MilliQ) immediately, and the cells were washed 4 times with purified water (MilliQ). Images were acquired under the microscope (Olympus, Tokyo, Japan) for analysis. After that, all the water

was removed and cells were dried completely. Oil red O dye was eluted with 100% isopropanol and incubated with gently shaking for 10 min. The OD values were measured at 490 nm using a multi-scan spectrum (Thermo Scientific, Waltham, MA, USA) with 100% isopropanol as a blank.

Total genomic DNA measurement

Genomic DNA was extracted from differentiated brown adipocytes following the manufacturer's instruction (Invitrogen). In brief, cells were collected and harvested by trypsin digestion at 37 °C for 5 min, centrifuged at 1500 rpm for 2 min, and the supernatant was removed. And then cells were re-suspended in 200 µL PBS, and 20 µL Proteinase K and 20 µL RNase A were added, and mixed well by brief vortexing and cells were incubated at room temperature for 2 min. 200 µL lysis buffer was added and mixed well by vortexing to obtain a homogenous solution. Then the samples were incubated at 55 °C for 10 min to promote protein digestion. Then, 200 µL ethanol was added and mixed well by vortexing to yield a homogenous solution. The genomic DNA purification was using a spin column-based centrifugation procedure. The lysate (~640 µL) prepared with lysis buffer and ethanol were added to the spin column, and the column was centrifuged at 10,000 rpm for 1 minute at room temperature, and then the collection was discarded and washed twice with washing buffer. Genomic DNA was eluted by using genomic elution buffer. The DNA amount was measured using a NanoDrop 1000 (Thermo Scientific, Waltham, MA, USA) absorbance at 260 nm.

Mechanical stimulation application

Mechanical stimulation was applied when medium was changed from the induction medium to the differentiation medium for 6 consecutive days to induce differentiation following a previous report [Shibasaki K et al., 2010]. A 3-D sunflower mini-shaker (Taitec, Koshigaya, Japan) was set in CO_2 incubator for generating mechanical force. Cell culture dishes (3.5 cm, BD Falcon, Austin, TX, USA) were put on the center, where the mechanical strength was weaker than the edge of the shaker. Therefore, I defined the mechanical strength on the center of the shaker is strength +, and that on the edge of the shaker is strength ++. The mini-shaker was set on the middle of the maxi-speed when applying a mechanical stimulation.

Histological analysis

Three or eight week-old WT and TRPV2KO male mice from same background were used for the histological study. iBAT tissues were fixed in 4% paraformaldehyde/PBS, embedded in paraffin wax and sectioned at 8 μm. In briefly, iBAT sections were first de-paraffinized in xylene for 20 min, and then treated with a gradient-decreased ethanol solution from 100% to 70%. The sections were stained in hematoxylin solution for 5 min and eosin solution for 10 min. Then the sections were immersed into a gradient-decreased ethanol solution from 100% to 70% following a dehydration process. The sections were finally penetrated with xylene for 5 min, 3 times, mounted and observed under the light microscopy (Keyence, Tokyo, Japan). Adipocyte sizes were assessed by measuring the diameter of lipid

droplets and adipocyte sizes using ImageJ software (National Institutes of Health, Bethesda, MD, USA).

In vivo temperature recording

Eight–week old mice from same background of WT or TRPV2KO mice were anesthetized with 2.0% isoflurane in 100% O_2 through a tracheal cannula with the animal's spontaneous ventilation. Each mouse was fixed on an electric heating pad to keep core body temperature among the range of 37 to 37.5 ^{o}C. Thermo-probes (Unique Medical, Japan) were inserted into the iBAT tissue and rectum. Recordings were started 20 min after the signals became stable. BRL37344 (600 μg/kg body weight) was administrated by intraperitoneally (i.p.). A Spike 2 software was used to obtain a continuous measurememt of iBAT, rectum and ambient temperatures.

Statistical analysis

Group data was represented as the mean ± SE. Statistical analysis was performed with Student's *t*-tests or one-way ANOVA followed by multiple *t*-tests with Bonferroni correction using Origin 8.5 software. Only two-tailed *P* values less than 0.05 were considered to be a significant difference.

3. Results

3.1 mRNA and protein of TRPV2 are expressed in the differentiated mouse brown adipocytes in culture

First of all, I checked TRPV2 expression in primary cultured brown adipocytes and BAT. RT-PCR and real-time PCR analyses revealed that expression level of *Trpv2* mRNA is the highest in the differentiated mouse brown adipocytes among *Trpv1*, *Trpv2, Trpv3* and *Trpv4* (Figure 1, A and B). And the same result was obtained in the analysis of mouse iBAT (Figure 1C). These results indicated that the *Trpv2* mRNA is dominantly expressed in mouse brown adipocytes. In addition, Western blot analysis of the immunoprecipitated samples demonstrated that TRPV2 protein was expressed in the differentiated brown adipocytes from wild-type (WT), but not TRPV2KO mice (Figure 1D). These results suggested that mRNA and protein of TRPV2 are expressed in the differentiated mouse brown adipocytes. Therefore, I aimed to explore the involvement of TRPV2 in mouse brown adipocytes.

Figure 1, near here

Next, I confirmed the functional expression of TRPV2 in mouse brown adipocytes using calcium-imagings and whole-cell patch-clamp recordings. A TRPV2 agonist, 2APB or LPC increased $[Ca^{2+}]_i$ which was blocked by a TRPV2-selective antagonist, SKF96365 (SKF) (Figure 2, A and B), indicating that the observed 2APB- or LPC-evoked $[Ca^{2+}]_i$ increases are mediated by TRPV2 activation. The result that the examined adipocytes showed increases in $[Ca^{2+}]_i$ upon NE application indicates that they are differentiated adipocytes. Ionomycin, an

ionophore, was used to confirm cell viability. These results revealed that TRPV2 is functionally expressed in the differentiated mouse brown adipocytes. Whole-cell patch-clamp recordings at -60 mV holding potential with ramp-pulses from -100 mV to +100 mV for 500 ms given every 5 s showed that 2APB activated inward currents with outward rectification which was blocked by SKF (Figure 2C). Mean densities of the 2APB-induced currents in mouse brown adipocytes at -60 mV and +100 mV were significantly smaller in the cells given both 2APB and SKF compared with cells given 2APB alone (Figure 2D). These results further suggested that TRPV2 is functionally expressed in mouse brown adipocytes.

Figure 2, near here

3.2 TRPV2 expression is dynamically changed during the differentiation of mouse brown adipocytes

Results thus far demonstrated that TRPV2 is functionally expressed in mouse brown adipocytes. In order to examine whether TRPV2 expression level is changed during the differentiation of mouse brown adipocytes, I examined the TRPV2 expression in pre-adipocytes, 2 day-differentiated brown adipocytes and 6 day-differentiated brown adipocytes of mice. First, I examined the mRNA and protein levels of TRPV2 in mouse brown adipocytes. Real-time RT-PCR results indicated that mRNA levels of TRPV2 are significantly increased in the 2 day- and 6 day-differentiated mouse brown adipocytes compared with pre-adipocytes. Moreover, there was no significant difference in the *Trpv2* mRNA levels between 2 day- and 6 day-differentiated mouse brown adipocytes (Figure 3A). Western blot experiments with the immune-

precipitated samples also revealed that protein levels of TRPV2 are elevated in the 2 day- and 6 day-differentiated mouse brown adipocytes compared with pre-adipocytes. Similar to the mRNA levels, there was no difference in TRPV2 protein levels between the 2 day- and 6 day-differentiated mouse brown adipocytes (Figure 3B). These results demonstrated that the mRNA and protein levels of TRPV2 are increased during the differentiation of mouse brown adipocytes.

I also examined the functional expression of TRPV2 in mouse brown adipocytes from different differentiation stages using a calcium-imaging method. Extent of the 2APB-evoked $[Ca^{2+}]_i$ increases were gradually elevated in pre-adipocytes (Figure 3C), 2 day-differentiated (Figure 3D) and 6 day-differentiated brown adipocytes (Figure 3E) as the differentiation progressed although ionomycin responses were somehow small in the 2 day-differentiated adipocytes. NE-evoked responses were also gradually increased in mouse brown adipocytes, supporting the progress of differentiation. Both 2APB- and NE-evoked responses normalized to the ionomycin responses were significantly increased in the differentiation process to similar extent indicated that the functional expression of TRPV2 paralleled the differentiation of the mouse brown adipocytes (Figure 3F).

I also compared sizes of the 2APB-evoked current responses in pre-adipocytes, 2 day-differentiated and 6 day-differentiated brown adipocytes, and found that the sizes were increased during the differentiation without changes in outward rectification (Figure 3G). Mean densities of the 2APB-activated currents at -60 mV and +100 mV were significantly increased in 2 day- and 6 day-differentiated mouse brown adipocytes compared with pre-adipocytes with a differentiation-dependent manner (Figure 3H). Furthermore, cell capacitances, reflecting the cell volume, were

also gradually increased during the differentiation of mouse brown adipocytes probably due to the accumulation of lipid droplets (Figure 3I). These all results indicated that functional expression of TRPV2 was dramatically increased during the differentiation of mouse brown adipocytes, suggesting that TRPV2 could be involved in the differentiation process of mouse brown adipocytes.

Figure 3, near here

3.3 TRPV2 activation prevents mouse brown adipocytes differentiation

To examine whether TRPV2 is involved in the differentiation of mouse brown adipocytes, I performed a pharmacological study by applying TRPV2 agonists with or without SKF. First, I tried to mimic the calcium influx by applying ionomycin to examine the effect of $[Ca^{2+}]_i$ increase on adipocyte differentiation because it has been reported that ionomycin-induced $[Ca^{2+}]_i$ increases inhibited 3T3-L1 cell differentiation [Ntambi JM and Takova T, 1996; Shi H, et al., 2000]. Ionomycin was applied when the medium was changed to the differentiation one. Ionomycin reduced the number of differentiated mouse brown adipocytes dose-dependently (Figure 4A), and about 60% reduction in the number of differentiated mouse brown adipocytes was caused by 0.3 μM of ionomycin (Figure 4B). These results suggested that $[Ca^{2+}]_i$ increases cause reduction in the mouse brown adipocyte differentiation.

Figure 4, near here

Next I tested the effects of a TRPV2 agonist, 2APB or LPC on the differentiation of mouse brown adipocytes. In this experiment, oil red O staining was performed because accumulated oil in the differentiated adipocytes can be visualized in the staining which makes the detection of differentiated cells much easier. 2APB or LPC was applied when the medium was changed to the differentiation one, and DMSO was added to differentiation medium as a control. The staining revealed that 2APB reduced the oil red O signals dose-dependently after 6-day differentiation of mouse brown adipocytes (Figure 5A). Thapsigargin (TG), a calcium pump inhibitor known to increase $[Ca^{2+}]_i$ similar to ionomycin, also reduced the oil red O signals [Jones KT and Sharpe GR, 1994], suggesting that $[Ca^{2+}]_i$ increases inhibit differentiation of mouse brown adipocytes. Analyses with different concentrations of 2APB or LPC showed that both 2APB and LPC reduced the number of differentiated mouse brown adipocytes in a dose-dependent manner and 2APB (100 μM) or LPC (10 μM) reduced about 40% of differentiated mouse brown adipocytes (Figure 5, B and C). Accordingly, these concentrations of TRPV2 agonists were used in the following experiments. These results suggested that TRPV2 activation-induced elevation of $[Ca^{2+}]_i$ prevents the mouse brown adipocytes differentiation.

Figure 5, near here

I also examined the effect of a TRPV2-selective antagonist, SKF [Ramsey IS et al., 2006; Juvin V et al., 2007] on the differentiation of mouse brown adipocytes. Co-application SKF (10 μM) significantly recovered the 2APB (100 μM)-induced inhibition of mouse brown adipocyte differentiation (Figure 6, A and B). SKF also significantly recovered the LPC (10 μM)-induced inhibition of mouse brown

adipocyte differentiation, further supporting the involvement of TRPV2 in the process. In addition, triglyceride levels were significantly decreased by 2APB and the reduction was recovered by SKF (Figure 6, B and C), supporting the concept that number of the differentiated mouse brown adipocytes are affected by TRPV2 activation. In these experiments, mouse brown adipocytes were treated with 2APB with or without SKF for 6 days in the differentiation medium. In order to examine whether TRPV2 activity-dependent regulation of the mouse brown adipocyte differentiation needs longer time, I treated the cells with chemicals for a longer time period (9 days), and essentially same results were obtained compared with the experiments with 6 days regarding the numbers of differentiated brown adipocytes and triglyceride levels (Figure 6, D and E). These results suggested that effects of TRPV2 activation are already saturated in the 6 day-treatment. To further confirm the effect of TRPV2 activation on mouse brown adipocyte differentiation, I analyzed the mRNA levels of UCP1 and PPARγ in the cells treated with 2APB or 2APB + SKF. Since UCP1 is specifically expressed in the mitochondrial inner membrane of the differentiated brown adipocytes [Arechaga et al., 2001] and PPARγ is a key transcriptional factor regulating fatty acid storage and glucose metabolism during the differentiation process [Varga T et al., 2011]. mRNA levels of both genes were significantly reduced by 2APB, and the reduction were significantly recovered by co-application of SKF (Figure 6, F and G). TG again reduced number of the differentiated brown adipocytes and mRNA levels of UCP1 and PPARγ, and induction medium did not affect any parameter reflecting adipocyte differentiation (Figure 6, B, C, E and F), supporting the reproducibility of the experiments.

Interpretation of the effects of 2APB, LPC and TG on the number of the differentiated brown adipocytes and on mRNA levels of UCP1 and PPARγ is based on the assumption that total cell numbers (differentiated and undifferentiated cells) are not changed. In order to exclude the possibility that TRPV2-mediated calcium influx induces apoptosis or cell death, which could also lead to the reduction in the differentiated brown adipocytes and triglyceride levels, I performed the total genomic DNA measurement. The total genomic DNA amounts were not changed by the treatment with 2APB, 2APB + SKF, LPC or ionomycin while total genomic DNA amounts of cells treated with induction medium were significantly elevated than cells in the differentiation medium (Figure 6H), demonstrating that pharmacological treatments did not cause cell death or apoptosis, and pre-adipocytes could be continuously proliferated in the induction medium. These results again suggested that TRPV2 activation prevented mouse brown adipocyte differentiation.

Figure 6, near here

3.4 Mechanical stimulation induced inhibition of mouse brown adipocytes differentiation via TRPV2 activation

It was reported that mechanical stimulation enhances the axon outgrowth via TRPV2 activation [Shibasaki K et al., 2010]. Following a previous paper, I applied mechanical stimulation during the differentiation procedure using a 3-D sunflower mini-shaker in the CO_2 incubator. Oil red O staining revealed that mechanical stimulation (both strength + and strength ++) inhibited mouse brown adipocyte differentiation and the reduction in the oil red O-positive differentiated adipocyte

numbers was greater in the adipocytes stimulated by mechanical strength ++ than by mechanical strength +. And this mechanical stimulation-induced inhibition of mouse brown adipocyte differentiation was rescued by co-application of SKF (Figure 7A). The oil red O staining results indicated that mechanical stimulation may inhibit mouse brown adipocyte differentiation via TRPV2 activation. Indeed, differentiated mouse brown adipocyte numbers and triglyceride levels were significantly reduced by mechanical stimulation in a strength-dependent manner, and the reduction was rescued by co-application of SKF (Figure 7, B and C). These results suggested that mechanical stimulation inhibited mouse brown adipocyte differentiation via TRPV2 activation.

Figure 7, near here

3.5 TRPV2 agonists inhibit mouse brown adipocytes differentiation more effectively in WT than in TRPV2KO adipocytes

In order to examine the involvement of TRPV2 in the differentiation of mouse brown adipocytes more clearly, I compared the differentiation of mouse brown adipocytes and the effects of 2APB or LPC on the brown adipocyte differentiation between WT and TRPV2KO mice. Oil red O staining experiments revealed that the basal levels of mouse brown adipocyte differentiation did not look different between adipocytes from the two genotypes. However, 2APB (100 μM) or LPC (10 μM) inhibited differentiation more effectively in WT than in TRPV2KO brown adipocytes (Figure 8A). Reduction in the differentiated brown adipocyte numbers and triglyceride levels by 2APB or LPC was greater in WT cells than in TRPV2KO cells while

reduction by ionomycin was not different (Figure 8, B and C). These results further suggested that chemical TRPV2 activation causes inhibition of mouse brown adipocyte differentiation.

Figure 8, near here

I also compared the effects of mechanical stimulation on the differentiation of mouse brown adipocytes from both two genotypes. Oil red O staining experiments revealed that mechanical stimulation inhibited the differentiation of WT brown adipocytes more effectively than TRPV2KO cells (Figure 9A). Differentiated brown adipocyte numbers and triglyceride levels were more greatly reduced in WT cells than in TRPV2KO cells although statistical significance was obtained in the experiments with strength ++ (Figure 9, B and C). These results further suggested that mechanical TRPV2 activation causes inhibition of mouse brown adipocyte differentiation.

Figure 9, near here

3.6 TRPV2 activation-induced inhibition of mouse brown adipocyte differentiation could involve a calcineurin pathway

It was reported that increased intracellular calcium levels by ionomycin inhibits the differentiation of adipocytes via a calcineurin activation, and subsequently inhibits the key transcriptional factors, PPARγ and C/EBPα, which further inhibit 3T3-L1 adipocyte differentiation [Neal JW and Clipstone NA, 2002]. A previous report also

demonstrated that calcium influx by activation of the "store-operated" Orai1 calcium channel in the plasma membrane upon Stim1 activation in endoplasmic reticulum (ER) inhibited 3T3-L1 adipocyte differentiation [Graham SJ et al., 2009]. In order to examine the involvement of a calcineurin pathway in the TRPV2-induced inhibition of the mouse brown adipocyte differentiation, I investigated the effects of FK506 or cyclosporine A (CsA), which suppress calciueurin activity. Reduction in both the number of differentiated brown adipocyte and triglyceride levels by either ionomycin, 2APB or LPC was significantly recovered by FK506 or CsA (Figure 10 A, B, C and D). These results suggested that TRPV2 activation-induced inhibition of mouse brown adipocyte differentiation involves a calcineurin pathway.

Figure 10, near here

3.7 TRPV2KO mice exhibit increases in brown adipocyte sizes of iBAT and impaired thermogenesis

As described above, I found membrane stretch-induced activation of TRPV2 inhibits mouse brown adipocyte differentiation via a calcineurin pathway *in vitro*. To check whether TRPV2 is involved in mouse iBAT differentiation *in vivo*, I analyzed TRPV2KO mice. TRPV2KO mice were generated as described in the method. I found that TRPV2KO mice exhibited significantly smaller body weight throughout the time course (Figure 11, A and B). Because iBAT from TRPV2KO mice had similar weighs compared with WT mice (Figure 11C), the iBAT weight per body weight was significantly larger in TRPV2KO mice than WT mice at both 3-week and 8-week of ages (Figure 11E), suggesting that TRPV2 is involved in the iBAT growth.

Figure 11, near here

To further explore the involvement of TRPV2 in the differentiation process of mouse iBAT, I performed the histological study by a hematoxylin and eosin staining experiment. iBAT was rich with capillary vessels and the cell nucleus was located at the periphery in adipocytes as reported [Prunet-Marcassus B et al., 1999; Chen Y et al., 2012]. Surprisingly, I observed more and larger unique lipid droplets rather than multiple lipid droplets in adipocytes from 3-week-old and 8-week-old TRPV2KO mice (Figure 12A). When comparing the droplet size distribution, mean values became significantly larger in TRPV2KO iBAT ($p < 0.01$) in 3-week-old and 2.47×10^{-6} in 8-week-old mice (12.2 ± 0.5 and 14.7 ± 0.2 μm in 3-week and 8-week old ages, respectively). While mean values in WT iBAT were small (9.1 ± 0.6 and 9.5 ± 0.2 μm in 3-week and 8-week old ages, respectively) (Figure 12B). In addition, cell diameters became distributed in larger ranges in TRPV2KO adipocytes than WT cells both at 3-week and 8-week of ages (Figure 12C), and mean diameters of TRPV2KO adipocytes were significantly larger than WT cells (14.9 ± 0.5 μm (3-week) and 15.8 ± 0.4 μm (8-week) in WT mice and 18.3 ± 0.5 μm (3-week) and 19.8 ± 0.3 μm (8-week) in TRPV2KO mice, $p < 0.01$ both at 3-week and 8-week of ages) (Figure 12D). These results can be explained to some extent by the loss of differentiation regulation in brown adipocytes lacking TRPV2.

Figure 12, near here

I asked whether over-grown larger adipocytes from TRPV2KO iBAT are as functional as WT cells. To address it, I examined the thermogenesis function of iBAT. Temperature increases in response to a β3-adrenergic receptor agonist BRL37344 in TRPV2KO iBAT were significantly smaller than those in WT iBAT ($1.45 \pm 0.27\ ^{o}C$ in TRPV2KO mice and $2.55 \pm 0.24\ ^{o}C$ in WT mice) (Figure 13A). Rectum temperature increases upon BRL37344 application were also significantly smaller in TRPV2KO mice than in WT mice ($0.95 \pm 0.23\ ^{o}C$ in TRPV2KO mice and $1.84 \pm 0.20\ ^{o}C$ in WT mice) with a slow time course (Figure 13B), which indicates that rectum temperatures changes follow iBAT temperatures changes.

Figure 13, near here

---

4. Discussion

In this study, I provided several lines of evidence that TRPV2 is functionally expressed in mouse brown adipocytes and acts as a mechano-sensor. I also showed that a TRPV2-mediated pathway negatively regulates mouse brown adipocyte differentiation. The results suggest that a mechano-sensor, TRPV2, could act as a brake for brown adipocyte differentiation, a key step in brown adipose tissue development. Lipid accumulation in the differentiated brown adipocytes could cause membrane stretch activating TRPV2 possibly to prevent over-growth which could lead to dysfunction of brown adipose tissue. Therefore, TRPV2 in brown adipocytes could be a promising therapy target for obesity.

Adipocytes play a number of key roles in systemic energy homeostasis and metabolic regulation [Ye L et al., 2012] and adipose tissue is the major contributor to obesity [Hajer GR et al., 2008]. It is well known that WAT is the primary depot for energy storage in mammals [Peeke PM & Chrousos GP. 1995] and that BAT is an important component in whole-body energy homeostasis through the dissipation of stored chemical energy in the form of heat [Lowell BB et al., 1997]. The role of BAT as a defense against both hypothermia and obesity, at least in rodents, is well established [Seale P et al., 2009]. Recently, it has been reported that BAT also exists in adult humans demonstrated by using a combination of high resolution imaging techniques [Cypess, AM et al., 2009; Van Marken Lichtenbelt, WD et al., 2009]. Therefore, the approaches modulating BAT function or differentiation possibly through TRPV2 could be intriguing ways for human obesity prevention and treatment.

Expression levels of TRPV2 were dramatically increased during the differentiation of mouse brown adipocytes not only in the mRNA and protein levels but also in its function analyzed using calcium-imaging and patch-clamp methods (Figures 1 - 3). It is interesting that TRPV2 expression levels are increased in the later stage of brown adipocyte differentiation (6 day-differentiated adipocytes) than in the early stages (pre-adipocytes and 2 day-differentiated adipocytes). Genome-wide binding analyses have revealed that many different genes were up-regulated during the differentiation of adipocytes due to PPARγ and C/EBPα cooperation on multiple binding sites in their promoter regions [Wu Z et al., 1999; Lowe CE et al., 2011]. Moreover, growth factors like insulin-like growth factor-1 were reported to up-regulate TRPV2 expression and function by inducing a dynamic and transient translocation of TRPV2 from intracellular compartments to the plasma membrane through a PI3K-dependent pathway [Kanzaki M et al., 1999; Boels K et al., 2001]. Thus, expression of TRPV2 could be somehow up-regulated in the late stage of differentiation to prevent brown adipocytes over-growth in a self-regulation manner although transcription and translation mechanisms of TRPV2 are still little known. In addition, the increased TRPV2 expression levels during the brown adipocyte differentiation could indicate that TRPV2 plays another role in brown adipocytes such as the brown adipocyte-dependent non-shivering thermogenesis.

Volume increases in adipocytes possibly due to lipid droplet accumulation could cause membrane stretch, which might be one major endogenous stimuli of TRPV2 activation. And some other endogenous stimuli, like growth factors, hormones, lipid metabolites, endocannabinoids and LPC could also activate TRPV2 and induce calcium influx [Kanzaki M et al., 1999; Boels K et al., 2001]. $[Ca^{2+}]_i$ increases upon

calcium influx either through TRPV2 activation or ionomycin inhibited differentiation of mouse brown adipocytes and diminished expression of the brown adipocyte-specific genes, UCP1 and PPARγ in the 6 day-differentiation process which is often used (Figures 4, 5 and 6). However, the fact that experiments for a longer time differentiation (9 day-differentiation) provided essentially same results with 6 day-differentiation (Figure 6) suggests that effects of TRPV2 inhibition occur only in the differentiation process, being consistent with a concept that differentiation of brown adipocytes is probably completed within six days [Irie Y et al., 1999; Klein J et al., 1999]. Moreover, TRPV2 activation-induced inhibition of brown adipocyte differentiation was recovered by FK506 and CsA (Figure 10). These observations are similar to those obtained in white adipocyte cell line, 3T3-L1 cells [Neal JW and Clipstone NA, 2002], suggesting that similar calcium signaling pathways are working both in white and brown adipocytes in the differentiation although TRPV2 involvement looks predominant in the brown adipocytes.

Differentiated adipocyte numbers and triglyceride levels in the isolated brown adipocytes from iBAT were not different in the 6 day-differentiation between WT and TRPV2KO mice, being not consistent with the concept that TRPV2 is activated by membrane stretch in the brown adipocytes and that the TRPV2 activation leads to the inhibition of adipocyte over-growth. These apparently unexpected results can be interpreted as TRPV2 in brown adipocytes is activated and involved in the regulation of brown adipocyte differentiation only under the *in vivo* condition. Alternatively, TRPV2 activation in brown adipocytes might not occur in a cell-autonomous manner. This interpretation could be supported by a previous report showing that TRPV2 knockdown did not trigger adipocyte differentiation in 3T3 adipocytes cell line [Ye L

et al., 2012]. Nevertheless, pharmacological experiments and mechanical stimulation experiments *in vitro* showed significant differences in brown adipocyte differentiation between the two genotypes, demonstrating that mechanical- or ligand-induced activation of TRPV2 is involved in the prevention of mouse brown adipocyte differentiation at least *in vitro* (Figures 8 and 9). The fact that mechanical- or ligand-induced activation of TRPV2 reduced the number of differentiated brown adipocytes and triglyceride levels both in WT and TRPV2KO adipocytes albeit to different extent suggests that other proteins including ion channels could also be involved in the prevention of mouse brown adipocyte differentiation. They could be other TRPV channels. Since *Trpv1*, *Trpv3* and *Trpv4* mRNA are expressed in mouse brown adipocytes (Figure 1) and 2APB also activates TRPV1 and TRPV3 [Hu HZ et al., 2004]. Moreover, mechanical stimulation activates not only TRPV2, but also TRPV4 [O'Neil RG and Heller S., 2005].

In the comparison between WT and TRPV2KO mice, the iBAT weight per body weight was significantly larger in TRPV2KO mice than WT mice at both 3-week and 8-week of ages (Figure 11E) and adipocyte size in iBAT from TRPV2KO mice was also significantly larger than cells from WT mice both at 3-week and 8-week of ages (Figure 12, F or G). This result seems consistent with the concept that TRPV2 functions as a break for brown adipocyte over-growth although cell number should be similar or even smaller in TRPV2KO adipocytes. Interestingly, lipid droplet sizes in TRPV2KO iBAT cells were also significantly larger than in WT cells and increased with ages (Figure 12, B and C). In addition, thermogenesis function of TRPV2KO iBAT in response to β3-adrenergic receptor stimulation was significant impaired compared with that of WT iBAT (Figure 13), suggesting that “whitening”

of brown adipocyte could be caused in TRPV2-KO mice. Similar phenomena were reported in other works showing that both aged and obese mice have iBAT abnormalities with increase in adipocyte sizes and reduction in thermogenesis ability [Sellayah D and Sikder D., 2014; Wahlig JL et al., 2012]. "Whitening" with reduced brown adipocyte function caused by over-growth could lead to impairment of thermogenesis. Although some reports suggest the involvement of non-selective cation channels in thermogenesis, it is not well established that the involvement of those channels in the regulation of gene expression related to thermogenesis and energy storage in adipose tissues and adipocytes. TRPM8 stimulation in brown adipocytes and BAT was reported to increase in UCP1 expression through Ca^{2+}-dependent PKA phosphorylation [Ma S et al., 2012] and disruption of TRPV4 protein was shown to enhance UCP1 and PGC1α gene expression in an adipocyte cell line and white adipocytes [Y Le et al., 2012]. Accordingly, I cannot exclude the possibility that TRPV2 is involved in thermogenesis. Nevertheless, it is an intriguing idea and a mechanism in brown adipose tissues which were not previously thought that the predominantly expressed TRPV2 channels act as a mechano-seosor for membrane stretch and negatively regulate brown adipocytes functions by optimizing brown adipocyte size and differentiation. In any case, further *in vitro* and *in vivo* analyses would be needed to confirm the concept.

I would like to propose a working model that shows the involvement of TRPV2 in the differentiation of mouse brown adipocytes (Figure 14). TRPV2-mediated inhibition of mouse brown adipocytes differentiation occurs via a calcineurin pathway. Ionomycin- or TG-induced $[Ca^{2+}]_i$ increases activate calcineurin via calcium-calmodulin (CaM) binding, and the activated calcineurin suppresses the key

adipogenesis transcriptional factors, PPARγ and C/EBPα, which further inhibits differentiation of mouse brown adipocytes. Membrane stretch-induced activation of TRPV2 also increases $[Ca^{2+}]_i$, which could prevent the differentiation of mouse brown adipocyte similarly via a calcineurin pathway. In conclusion, my study establishes a novel role for mechano-sensitive TRPV2 in mouse brown adipocyte differentiation. In brown adipocytes, TRPV2 activation due to membrane stretch through lipid droplet accumulation might be necessary for preventing brown adipocyte over-growth and maintaining iBAT function under physiological condition, and regulation of TRPV2 function would be a promising therapeutic approach for preventing and combating human obesity and related metabolic disorders.

Figure 14, near here

---

5. References

Ahn J, Lee H, Kim S, Park J, Ha T. The anti-obesity effect of quercetin is mediated by the AMPK and MAPK signaling pathways. Biochemical and Biophysical Research Communications. 2008. 373(4): p. 545-549.

Pi-Sunyer FX. The Obesity Epidemic: Pathophysiology and Consequences of Obesity. Obesity. 2002. 10(S12): p. 97S-104S.

Hajer GR, van Haeften TW, Visseren FL. Adipose tissue dysfunction in obesity, diabetes, and vascular diseases. Eur Heart J. 2008; 29(24): 2959-2971.

Lowell BB, Flier JS. Brown adipose tissue, beta 3-adrenergic receptors, and obesity. Annu Rev Med. 1997; (48): 307-316.

Cannon B, Nedergaard J. Brown adipose tissue: function and physiological significance. Physiol Rev. 2004; 84(1): 277-359.

Argyropoulos G, Harper ME. Uncoupling proteins and thermoregulation. J Appl Physiol. 2002; 92(5): 2187-2198.

Mozo J, Emre Y, Bouillaud F, Ricquier D, Criscuolo F. Thermoregulation: what role for UCPs in mammals and birds? Biosci Rep. 2005; 25(3-4): 227-249.

Cypess AM, Lehman S, Williams G, Tal I, Rodman D, Goldfine AB, Kuo FC, Palmer EL, Tseng YH, Doria A, Kolodny GM, Kahn CR. Identification and importance of brown adipose tissue in adult humans. N Engl J Med. 2009; (360): 1509–1517.

Van Marken Lichtenbelt WD, Vanhommerig JW, Smulders NM, Drossaerts JM, Kemerink GJ, Bouvy ND, Schrauwen P, Teule GJ. Cold-activated brown adipose tissue in healthy men. N Engl J Med. 2009; (360): 1500–1508.

Ghosh A, Greenberg ME. Calcium signaling in neurons: molecular mechanisms and cellular consequences. Science. 1995; 268(5208): 239-247.

Michael J, Berridge, Martin D, Bootman & H Llewelyn Roderick. Calcium signalling: dynamics, homeostasis and remodeling. Nat Rev Mol Cell Biol. 2003; 4(7): 517-529.

Ntambi JM, Takova T. Role of Ca2+ in the early stages of murine adipocyte differentiation as evidenced by calcium mobilizing agents. Differentiation. 1996; (60): 151–158.

Shi H, Halvorsen YD, Ellis PN, Wilkison WO, Zemel MB. Role of intracellular calcium in human adipocyte differentiation. Physiol Genomics. 2000; 3(2): 75-82.

Jones KT, Sharpe GR. Thapsigargin raises intracellular free calcium levels in human keratinocytes and inhibits the coordinated expression of differentiation markers. Exp Cell Res. 1994; 210(1): 71-76.

Neal JW, Clipstone NA. Calcineurin mediates the calcium-dependent inhibition of adipocyte differentiation in 3T3-L1 cells. J. Biol. Chem. 2002; (277): 49776–49781.

Neal JW, Clipstone NA. A constitutively active NFATc1 mutant induces a transformed phenotype in 3T3-L1 fibroblasts. J. Biol. Chem. 2003; (278): 17246–17254.

Mathieu RL, Casez JP, Jaeger P, Montandon A, Peheim E, Horber FF. Altered body composition and fuel metabolism in stable kidney transplant patients on immuno-suppressive monotherapy with cyclosporine A. Eur J Clin Invest. 1994; (24): 195–200.

Berridge MJ. Calcium microdomains: organization and function. Cell Calcium. 2006; (40): 405–412.

Graham SJ, Black MJ, Soboloff J, Gill DL, Dziadek MA, Johnstone LS. Stim1, an endoplasmic reticulum Ca2+ sensor, negatively regulates 3T3-L1 pre-adipocyte differentiation. Differentiation. 2009; 77(3): 239-247.

Montell C, Rubin GM. Molecular characterization of the Drosophila trp locus: a putative integral membrane protein required for phototransduction. Neuron. 1989; 2(4): 1313-1323.

Shigematsu H, Sokabe T, Danev R, Tominaga M, Nagayama K. A 3.5-nm Structure of Rat TRPV4 Cation Channel Revealed by Zernike Phase-contrast Cryoelectron Microscopy. J Biol Chem. 2010; 285(15): 11210-11218.

Moiseenkova-Bell VY, Stanciu LA, Serysheva II, Tobe BJ, Wensel TG. Structure of TRPV1 channel revealed by electron cryomicroscopy. Proc Natl Acad Sci U S A. 2008; 105(21): 7451-7455.

Caterina MJ, Schumacher MA, Tominaga M, Rosen TA, Levine JD, Julius D. The capsaicin receptor: a heat-activated ion channel in the pain pathway. Nature. 1997; 389(6653): 816-824.

Tominaga M, Caterina MJ, Malmberg AB, Rosen TA, Gilbert H, Skinner K, Raumann BE, Basbaum AI, Julius D. The cloned capsaicin receptor integrates multiple pain-producing stimuli. Neuron. 1998; 21(3): 531-543.

Link TM, Park U, Vonakis BM, Raben DM, Soloski MJ, Caterina MJ. TRPV2 has a pivotal role in macrophage particle binding and phagocytosis. Nat Immunol. 2010; 11(3): 232-239.

Uchida K, Dezaki K, Damdindorj B, Inada H, Shiuchi T, Mori Y, Yada T, Minokoshi Y, Tominaga M. Lack of TRPM2 impaired insulin secretion and glucose metabolisms in mice. Diabetes. 2011; 60(1): 119-126.

Story GM, Peier AM, Reeve AJ, et al. ANKTM1, a TRP-like channel expressed in nociceptive neurons, is activated by cold temperatures. Cell. 2003; 112(6): 819-829.

Perálvarez-Marín, A.; Doñate-Macian, P.; Gaudet, R. What do we know about the transient receptor potential vanilloid 2 (TRPV2) ion channel? FEBS J. 2013; (280): 5471–5487.

Caterina, M.J, Rosen, T.A, Tominaga, M, Brake, A.J, Julius, D. A capsaicin-receptor homologue with a high threshold for noxious heat. Nature. 1999; (398): 436–441.

Juvin V, Penna A, Chemin J, Lin YL, Rassendren FA. Pharmacological characterization and molecular determinants of the activation of transient receptor potential V2 channel orthologs by 2-aminoethoxydiphenyl borate. Mol Pharmacol. 2007; 72(5): 1258-1268.

Monet M, Gkika D, Lehen'kyi V, Pourtier A, Vanden Abeele F, Bidaux G, Juvin V, Rassendren F, Humez S, Prevarsakaya N. Lysophospholipids stimulate prostate cancer cell migration via TRPV2 channel activation. Biochim Biophys Acta. 2009; 1793(3): 528-539.

Ramsey IS, Delling M, Clapham DE. An introduction to TRP channels. Annu Rev Physiol. 2006; (68): 619-647.

Muraki K, Iwata Y, Katanosaka Y, Ito T, Ohya S, Shigekawa M, Imaizumi Y. TRPV2 is a component of osmotically sensitive cation channels in murine aortic myocytes. Circ Res. 2003; 93(9): 829-838.

Iwata Y, Katanosaka Y, Arai Y, Shigekawa M, Wakabayashi S. Dominant-negative inhibition of Ca2+ influx via TRPV2 ameliorates muscular dystrophy in animal models. Hum Mol Genet. 2009; 18(5): 824-834.

Mihara H, Boudaka A, Shibasaki K, Yamanaka A, Sugiyama T, Tominaga M. Involvement of TRPV2 activation in intestinal movement through nitric oxide production in mice. J Neurosci. 2010; 30(49): 16536-16544.

Shibasaki K, Murayama N, Ono K, Ishizaki Y, Tominaga M. TRPV2 enhances axon outgrowth through its activation by membrane stretch in developing sensory and motor neurons. J Neurosci. 2010; 30(13): 4601-4612.

Irie Y, Asano A, Cañas X, Nikami H, Aizawa S, Saito M. Immortal brown adipocytes from p53-knockout mice: differentiation and expression of uncoupling proteins. Biochem Biophys Res Commun. 1999; 255(2): 221-225.

Arechaga I, Ledesma A, Rial E. The mitochondrial uncoupling protein UCP1: a gated pore. IUBMB Life. 2001; 52(3-5): 165-173.

Varga T, Czimmerer Z, Nagy L. PPARs are a unique set of fatty acid regulated transcription factors controlling both lipid metabolism and inflammation. Biochim Biophys Acta. 2011; 1812(8): 1007-1022.

Prunet-Marcassus B, Moulin K, Carmona MC, Villarroya F, Pénicaud L, Casteilla L. Inverse distribution of uncoupling proteins expression and oxidative capacity in mature adipocytes and stromal-vascular fractions of rat white and brown adipose tissues. FEBS Lett. 1999; 464(3): 184-188.

Chen YI, Cypess AM, Sass CA, Brownell AL, Jokivarsi KT, Kahn CR, Kwong KK. Anatomical and functional assessment of brown adipose tissue by magnetic resonance imaging. Obesity (Silver Spring). 2012; 20(7): 1519-1526.

Ye L, Kleiner S, Wu J, Sah R, Gupta RK, Banks AS, Cohen P, Khandekar MJ, Boström P, Mepani RJ, Laznik D, Kamenecka TM, Song X, Liedtke W, Mootha VK, Puigserver P, Griffin PR, Clapham DE, Spiegelman BM. TRPV4 is a regulator of adipose oxidative metabolism, inflammation, and energy homeostasis. Cell. 2012; 151(1): 96-110.

Peeke PM, Chrousos GP. Hypercortisolism and obesity. Ann N Y Acad Sci. 1995; (29)771: 665-676.

Seale P, Kajimura S, Spiegelman BM. Transcriptional control of brown adipocyte development and physiological function--of mice and men. Genes Dev. 2009; 23(7): 788-797.

Wu Z, Rosen ED, Brun R, Hauser S, Adelmant G, Troy AE, McKeon C, Darlington GJ, Spiegelman BM. Cross-regulation of C/EBP alpha and PPAR gamma controls the transcriptional pathway of adipogenesis and insulin sensitivity. Mol Cell. 1999; 3(2): 151-158.

Lowe CE, O'Rahilly S, Rochford JJ. Adipogenesis at a glance. J Cell Sci. 2011; 124(Pt 16): 2681-2686.

Kanzaki M, Zhang Y.Q, Mashima H, Li L, Shibata H, Kojima I. Translocation of a calcium-permeable cation channel induced by insulin-like growth factor-I. Nat. Cell. Biol. 1999; (1): 165–170.

Boels K, Glassmeier G, Herrmann D, Riedel I.B, Hampe W, Kojima I, Schwarz J.R, Schaller H.C. The neuropeptide head activator induces activation and translocation of the growth factor-regulated Ca(2+)-permeable channel GRC. J. Cell Sci. 2001; (114); 3599–3606.

Klein J, Fasshauer M, Ito M, Lowell BB, Benito M, Kahn CR. beta(3)-adrenergic stimulation differentially inhibits insulin signaling and decreases insulin-induced glucose uptake in brown adipocytes. J Biol Chem. 1999; 274(49): 34795-34802.

Iwata Y, Katanosaka Y, Arai Y, Shigekawa M, Wakabayashi S. Dominant-negative inhibition of Ca2+ influx via TRPV2 ameliorates muscular dystrophy in animal models. Hum Mol Genet. 2009; 18(5): 824-834.

Muraki K, Iwata Y, Katanosaka Y, Ito T, Ohya S, Shigekawa M, Imaizumi Y. TRPV2 is a component of osmotically sensitive cation channels in murine aortic myocytes. Circ Res. 2003; 93(9): 829-838.

Hu HZ, Gu Q, Wang C, Colton CK, Tang J, Kinoshita-Kawada M, Lee LY, Wood JD, Zhu MX. 2-aminoethoxydiphenyl borate is a common activator of TRPV1, TRPV2, and TRPV3. J Biol Chem. 2004; 279(34): 35741-35748.

O'Neil RG, Heller S. The mechanosensitive nature of TRPV channels. Pflugers Arch. 2005; 451(1): 193-203.

Sellayah D, Sikder D. Orexin restores aging-related brown adipose tissue dysfunction in male mice. Endocrinology. 2014; 155(2): 485-501.

Wahlig JL, Bales ES, Jackman MR, Johnson GC, McManaman JL, Maclean PS. Impact of high-fat diet and obesity on energy balance and fuel utilization during the metabolic challenge of lactation. Obesity (Silver Spring). 2012; 20(1): 65-75.

Bégin-Heick N. Beta 3-adrenergic activation of adenylyl cyclase in mouse white adipocytes: modulation by GTP and effect of obesity. J Cell Biochem. 199; 58(4): 464-473.

Ma S, Yu H, Zhao Z, Luo Z, Chen J, Ni Y, Jin R, Ma L, Wang P, Zhu Z, Li L, Zhong J, Liu D, Nilius B, Zhu Z. Activation of the cold-sensing TRPM8 channel triggers UCP1-dependent thermogenesis and prevents obesity. J Mol Cell Biol. 2012; 4(2): 88-96.

6. Figure Legends

Table 1. Sequences of the primers used for RT-PCR and Real-time RT-PCR

Figure 1. mRNA and protein of TRPV2 are expressed in the differentiated mouse brown adipocytes

A Representative results for RT-PCR experiments using differentiated mouse brown adipocytes. RT-PCR results of β-actin, *Trpv1*, *Trpv2*, *Trpv3* and *Trpv4* using differentiated mouse brown adipocytes after 29 (upper) and 35 (lower) thermal cycles are shown. Control (Ct.) lanes indicate the results with each vector as a template. **B** Results for real-time PCR of *Trpv1*, *Trpv2*, *Trpv3* and *Trpv4* using mouse pre-adipocytes and differentiated brown adipocytes. The mRNA expression levels were normalized to that 36B4 (ribosomal protein) mRNA. 36B4 is a housekeeping gene whose expression is un-affected by adipogenesis. Mean ± SE, n = 6. **C** Results for real-time PCR of *Trpv1*, *Trpv2*, *Trpv3* and *Trpv4* using mouse interscapular brown adipose tissue. The mRNA expression levels were normalized to that of 36B4 mRNA. Mean ± SE, n = 5. **D** A Western blot result of the immunoprecipitated samples from wild-type (WT) and TRPV2-deficient (TRPV2 KO) differentiated mouse brown adipocytes probed with antibodies against TRPV2 and tubulin. An upper band in TRPV2 blot likely indicates a glycosylated form.

Figure 2. TRPV2 is functionaly expressed in the differentiated mouse brown adipocytes

A and **B**, Responses evoked by a TRPV2 agonist, 2APB (A) or LPC- (B) were blocked by a selective TRPV2 antagonist SKF. NE-evoked responses indicate that examined brown adipocytes are differentiated ones. Ionomycin was used to confirm cell viability. Ratio values correspond to the real $[Ca^{2+}]_i$ of differentiated mouse brown adipocytes. **C** A representative whole-cell current activated by a TRPV2 agonist, 2APB, was inhibited by a TRPV2-selective antagonist, SKF in the differentiated mouse brown adipocytes. A voltage ramp-pulse protocol (500 ms) shown in the inset (upper left). Current-voltage curves of basal currents (black), currents in the presence of 2APB+SKF (blue) and currents in the presence of 2APB alone (red) at the time points of a, b and c, respectively, in the differentiated mouse brown adipocytes are shown in the inset (upper right). **D** Comparison of the mean densities of basal currents (black), currents in the presence of 2APB+SKF (blue) and currents in the presence of 2APB alone (red) at -60 mV and +100 mV in the differentiated mouse brown adipocytes. Mean ± SE, n = 10, ** $P < 0.01$ and n.s. (not significant) vs. base, $^{\#\#}$ $P < 0.01$ vs. 2APB alone. One-way ANOVA followed by 2-tailed *t*-test with Bonferroni correction.

Figure 3. Functional expression of TRPV2 is dynamically changed during the differentiation process of mouse brown adipocytes

A A real-time PCR result of *Trpv2* in pre-adipocytes, 2 day-differentiated brown adipocytes and 6 day-differentiated brown adipocytes. Mean ± SE, n = 6, * $P < 0.05$ vs. pre-adipocytes, n.s. vs. 2 day-differentiated adipocytes. One-way ANOVA followed by 2-tailed *t*-test with Bonferroni correction. **B** Western blot results of the immunoprecipitated samples with antibodies against TRPV2 and tubulin from pre-

adipocytes, 2 day-differentiated brown adipocytes and 6 day-differentiated brown adipocytes. An upper band in TRPV2 blot likely indicates a glycosylated form. **C**, **D** and **E** Figures show each individual trace of $[Ca^{2+}]_i$ changes in response to 2APB in pre-adipocytes (C), 2 day-differentiated brown adipocytes (D) and 6 day-differentiated brown adipocytes (E) of mice. NE-evoked responses indicate that cells are differentiated brown adipocytes. Ionomycin was used to confirm cell viability. Ratio values correspond to the real $[Ca^{2+}]_i$ of differentiated mouse brown adipocytes. **F** Averaged ratio values in response to 2APB or NE normalized to that induced by ionomycin in mouse brown adipocytes from pre-adipocytes (black), 2 day-differentiated brown adipocytes (blue) and 6 day-differentiated brown adipocytes (red). Mean ± SE, n = 218-870, ** $P < 0.01$ vs. pre-adipocytes, $^{\#}$ $P < 0.05$ vs. 2 days differentiated adipocytes. One-way ANOVA followed by 2-tailed *t*-test with Bonferroni correction. **G** Representative traces of the currents in response to 2APB in pre-adipocytes (black), 2 day-differentiated brown adipocytes (blue) and 6 day-differentiated brown adipocytes (red) of mice. Current-voltage curves of the current responses at the time points indicated by a, b and c are shown in the inset. **H** Comparison of the mean densities of currents from pre-adipocytes (black), 2 day-differentiated brown adipocytes (blue) and 6 day-differentiated brown adipocytes (red) of mice in response to 2APB at -60 mV and +100 mV. **I** Comparison of cell capacitance of pre-adipocytes (black), 2 day-differentiated brown adipocytes (blue) and 6 day-differentiated brown adipocytes (red) of mice. Mean ± SE, n = 13-17, * $P < 0.05$ and ** $P < 0.01$ vs. pre-adipocytes, $^{\#}$ $P < 0.05$, $^{\#\#}$ $P < 0.01$ vs. 2 day-differentiated adipocytes. One-way ANOVA followed by 2-tailed *t*-test with Bonferroni correction.

Figure 4. Ionomycin induced reduction in the number of differentiated mouse brown adipocytes in a dose-dependent manner

A Representative images of the differentiated mouse brown adipocytes after 6 day-differentiation in a differentiation medium applied with different doses of ionomycin. Scale bar indicates 100 μm. **B** A dose-dependency of the ionomycin-induced reduction in the number of differentiated mouse brown adipocytes. About 60% reduction in the number of differentiated mouse brown adipocytes was caused by 0.3 μM of ionomycin. Mean ± SE, n = 6, * $P < 0.05$ and ** $P < 0.01$ vs. control group. One-way ANOVA followed by 2-tailed *t*-test with Bonferroni correction.

Figure 5. A TRPV2 agonist, 2APB or LPC reduced the number of differentiated mouse brown adipocytes in a dose-dependent manner

A Oil red O staining images of 2APB- or thapsigargin-induced reduction in the oil red O signals of differentiated mouse brown adipocytes. DMSO was added to the differentiation medium as a control. Scale bar indicates 100 μm. **B** and **C** Dose-depend reduction in the number of differentiated mouse brown adipocytes treated with 2APB (B) or LPC (C). Thapsigargin (TG) also showed the dose-dependent reduction in the number of differentiated mouse brown adipocytes (B). 2APB 100 μM or LPC 10μM caused around 40% reduction in the number of differentiated mouse brown adipocytes. Mean ± SE, n = 6, * $P < 0.05$ and ** $P < 0.01$ vs. control group. One-way ANOVA followed by 2-tailed *t*-test with Bonferroni correction.

Figure 6. TRPV2 activation prevents differentiation of mouse brown adipocytes

A Oil red O staining images upon application of 2APB (100 μM) with or without a TRPV2- selective antagonist, SKF (10 μM) in the differentiation medium. Scale bar indicates 100 μm. **B** and **C** Numbers of 6 day-differentiated mouse brown adipocytes (B) and triglyceride levels (C) upon various pharmacological treatments. 2APB (100 μM), SKF (10 μM), TG (30 nM). **D** and **E** Numbers of 9 day-differentiated (9 day-diff.) mouse brown adipocytes (D) and triglyceride levels (E) upon various pharmacological treatments. Ionomycin (Iono.) (0.3 μM). **F** and **G** *Ucp1* (F) and *Pparγ* (G) mRNA levels upon various pharmacological treatments in the 6 day-differentiated mouse brown adipocytes. **H** Total genomic DNA amounts per well after various pharmacological treatments in 6 day-differentiated mouse brown adipocytes. Mean ± SE, n = 6 (n=8 in D and E), ** $P < 0.05$ and ** $P < 0.01$ vs control group, # $P < 0.05$ vs. 2APB or LPC group, n.s. vs. control group. One-way ANOVA followed by 2-tailed *t*-test with Bonferroni correction.

Figure 7. Mechanical stimulation induced inhibition of mouse brown adipocyte differentiation via TRPV2 activation

A Oil red O staining images of the 6 day-differentiated mouse brown adipocytes with or without mechanical stimulation. Scale bar indicates 100 μm. **B** and **C** Numbers of 6 day-differentiated mouse brown adipocytes (B) and triglyceride levels (C) upon mechanical stimulation. Mechanical strength ++ is stronger than mechanical strength +. Mean ± SE, n = 5, * $P < 0.05$ and ** $P < 0.01$ vs. control group, # $P < 0.05$ vs. strength ++ group. One-way ANOVA followed by 2-tailed *t*-test with Bonferroni correction.

Figure 8. TRPV2 agonists inhibit mouse brown adipocytes differentiation more effectively in WT than in TRPV2KO adipocytes

A Oil red O staining images of the 6 day-differentiated mouse brown adipocytes from WT and TRPV2KO mice with application of 2APB or LPC. Scale bar indicates 100 μm. **B** and **C** Comparison of the numbers of 6 day-differentiated mouse brown adipocytes (B) and triglyceride levels (C) in the cells from WT and TRPV2KO mice. Black bars indicate data collected from WT mice, and red bars indicate data collected form TRPV2KO mice. Mean ± SE, n=9, 3 weeks old mice, male. * $P < 0.05$ vs. control group, # $P < 0.05$. One-way ANOVA followed by 2-tailed *t*-test with Bonferroni correction.

Figure 9. Mechanical stimulation inhibits the differentiation of WT brown adipocytes more effectively than TRPV2KO cells

A Oil red O staining images of the 6 day-differentiated mouse brown adipocytes from WT and TRPV2KO mice with or without mechanical stimulation. Scale bar indicates 100 μm. **B** and **C** Comparison of the numbers of 6 day-differentiated mouse brown adipocytes (B) and triglyceride levels (C) in the cells from WT and TRPV2KO mice. Black bars indicate data collected from WT mice, and red bars indicate data collected from TRPV2KO mice. Mean ± SE, n=9, 3 weeks old mice, male. * $P < 0.05$ vs control group, # $P < 0.05$. One-way ANOVA followed by 2-tailed *t*-test with Bonferroni correction.

Figure 10. FK506 and cyclosporine A recover TRPV2 activation-induced inhibition of mouse brown adipocyte differentiation

A and **B** Effects of FK506 on the numbers of 6 day-differentiated mouse brown adipocytes (A) and triglyceride levels (B) upon various pharmacological treatments. Ionomycin (0.3 μM), 2APB (100 μM), LPC (10 μM), FK506 (5 μM). **C** and **D** Effects of cyclosporine A (CsA) on the numbers of 6 day-differentiated mouse brown adipocytes (C) and triglyceride levels (D) upon various pharmacological treatments. Ionomycin (0.3 μM), 2APB (100 μM), LPC (10 μM), CsA (1 μM). Mean ± SE, n=6, * $P < 0.05$ vs. control group, # $P < 0.05$. One-way ANOVA followed by 2-tailed *t*-test with Bonferroni correction.

Figure 11. TRPV2KO mice phenotype

A Representative pictures of WT and TRPV2KO 8-week old male mice. **B** Body weight changes from 3-week to 8-week of ages between the two genotypes (n=11). **C** Representative pictures of iBAT from WT and TRPV2KO mice. **D** and **E** The iBAT weight (D) and iBAT weight per mouse body weight ratio (E) of WT and TRPV2KO mice (n=6). Mean ± SE, * $P < 0.05$ vs. WT group, ** $P < 0.01$ vs. WT group. Unpaired Student's *t*-test.

Figure 12. Comparison of adipocyte sizes between WT and TRPV2KO iBAT

A Representative morphological results of iBAT by hematoxylin and eosin staining from 3-week and 8-week WT and TRPV2KO mice. Scale bar indicates 100 μm. **B** Comparison of lipid droplet size histograms from 3-week (left) and 8-week (right) old WT (Black) and TRPV2KO (Red) iBAT with hematoxylin and eosin staining.

Mean values are 9.1 ± 0.6 and 9.5 ± 0.2 μm in 3-week and 8-week old WT adipocytes, and 12.2 ± 0.5 and 14.7 ± 0.2 μm in 3-week and 8-week old TRPV2KO adipocytes. **C** Comparison of adipocyte size histograms from 3-week (left) and 8-week (right) old WT (Black) and TRPV2KO (Red) iBAT with hematoxylin and eosin staining. Mean values are 14.9 ± 0.5 and 15.8 ± 0.4 μm in 3-week and 8-week old WT adipocytes, and 18.3 ± 0.5 and 19.8 ± 0.3 μm in 3-week and 8-week old TRPV2KO adipocytes. **D** Mean diameters of adipocytes 3-week (left) or 8-week (right) in WT mice (Black) and TRPV2KO mice (Red). Mean ± SE, n=4. ** $P <$ 0.01 vs. WT group. Unpaired Student's *t*-test.

Figure 13. Comparison of thermogenetic function between WT and TRPV2KO mice

A and **B** Average traces of changes in iBAT temperature (A) or rectum body temperature (B) from WT and TRPV2KO mice after a BRL37344 (600 μg/kg body weight) administration (i.p., arrows). Mean ± SE, n=5, * $P < 0.05$ vs. WT group. Unpaired Student's *t*-test.

Figure 14. TRPV2-mediated inhibition of mouse brown adipocytes differentiation occurs via a calcineurin pathway

A working-model shows the involvement of TRPV2 in the differentiation of mouse brown adipocytes. Ionomycin- or TG-induced $[Ca^{2+}]_i$ increases activate calcineurin via calcium-calmodulin binding, and the activated calcineurin suppresses the key transcriptional factors, PPARγ and C/EBPα, which further inhibits differentiation of mouse brown adipocytes. Membrane stretch-induced activation of TRPV2 also

increases $[Ca^{2+}]_i$, which could prevent the differentiation of mouse brown adipocyte similarly via a calcineurin pathway.

7. Table and figures

Table 1. Sequences of the primers for RT-PCR and Real-time RT-PCR

Gene	Forward primer (5'-3')	Reverse primer (5'-3')	Annealing Temp.	Expected size
For RT-PCR				
TRPV1	AACTCCACCCCACACTGAAG	TCGCCTCTGCAGGAAATACT	60°C	548 bp
TRPV2	ACCGCATGGTGGTTTTAGAG	CTACAGCAAAGCCGAAAAGG	60°C	552 bp
TRPV3	CCCCATCCTCTTTCTCTTCC	CGACGTTTCTGGGAATTCAT	60°C	421 bp
TRPV4	ACAACACCCGAGAGAACACC	CCCAAACTTACGCCACTTGT	60°C	404 bp
β-actin	TGTTACCAACTGGGACGACA	AAGGAAGGCTGGAAAAGAGC	60°C	572 bp
For Real-time RT-PCR				
TRPV1	TGACAGCGAGTTCAAAGACCCAGA	GGCATTGACAAACTGCTTCAGGCT	57°C	145 bp
TRPV2	AGCACACAGGCATCTACAGTGTCA	TTACTAGGGCTACAGCAAAGCCGA	57°C	111 bp
TRPV3	AGCCAGGACCATCTTGGAGTTTGA	TTCCGTCCACTTCACCTCGTTGAT	57°C	136 bp
TRPV4	ACAACACCCGAGAGAACACCAAGT	GAGGCGAAAGGCCATCATTGTTGA	57°C	122 bp
UCP1	TACCAAGCTGTGCGATGTCCA	GCACACAAACATGATGACGTTCC	57°C	92 bp
PPARγ	GTGCCAGTTTCGATCCGTAGA	GGCCAGCATCGTGTAGATGA	53°C	141 bp
36B4	GGCCCTGCACTCTCGCTTTC	TGCCAGGACGCGCTTGT	57°C	123 bp

Figure 1

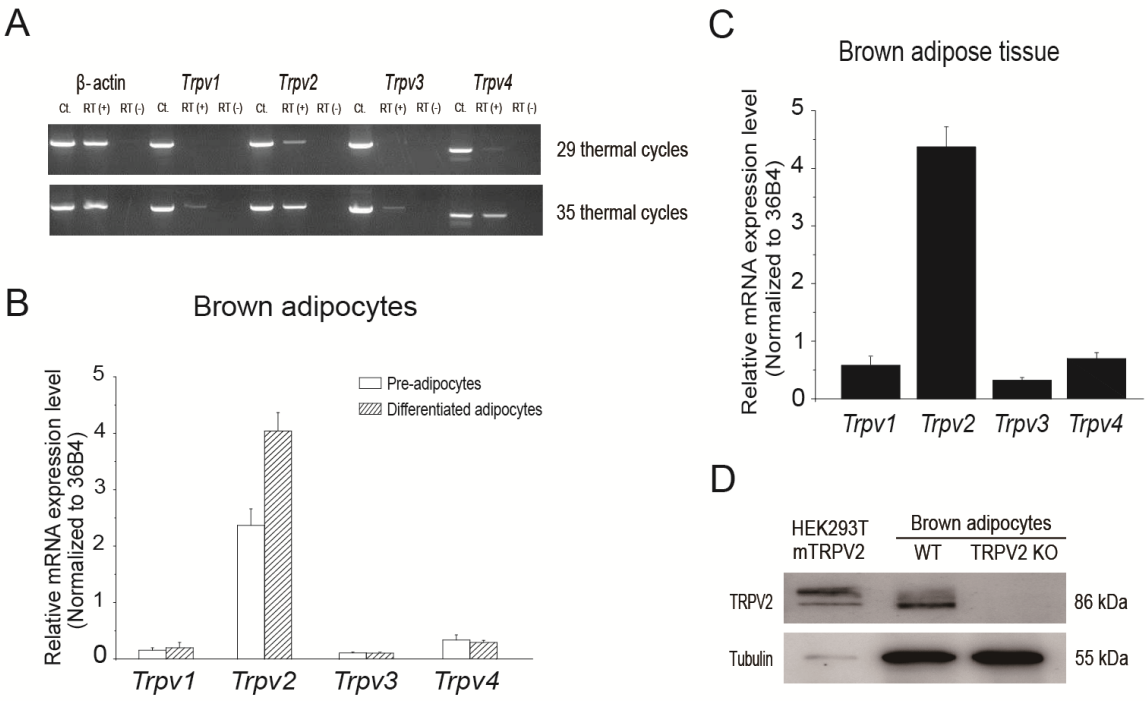
A
β-actin
Trpv1
Trpv2
Trpv3
Trpv4
Ct. RT (+) RT (-) Ct. RT (+) RT (-) Ct. RT (+) RT (-) Ct. RT (+) RT (-) Ct. RT (+) RT (-)
29 thermal cycles
35 thermal cycles
B
Brown adipocytes
Relative mRNA expression level (Normalized to 36B4)
Pre-adipocytes
Differentiated adipocytes
Trpv1 Trpv2 Trpv3 Trpv4
C
Brown adipose tissue
Relative mRNA expression level (Normalized to 36B4)
Trpv1 Trpv2 Trpv3 Trpv4
D
HEK293T mTRPV2
Brown adipocytes
WT
TRPV2 KO
TRPV2
86 kDa
Tubulin
55 kDa

Figure 2

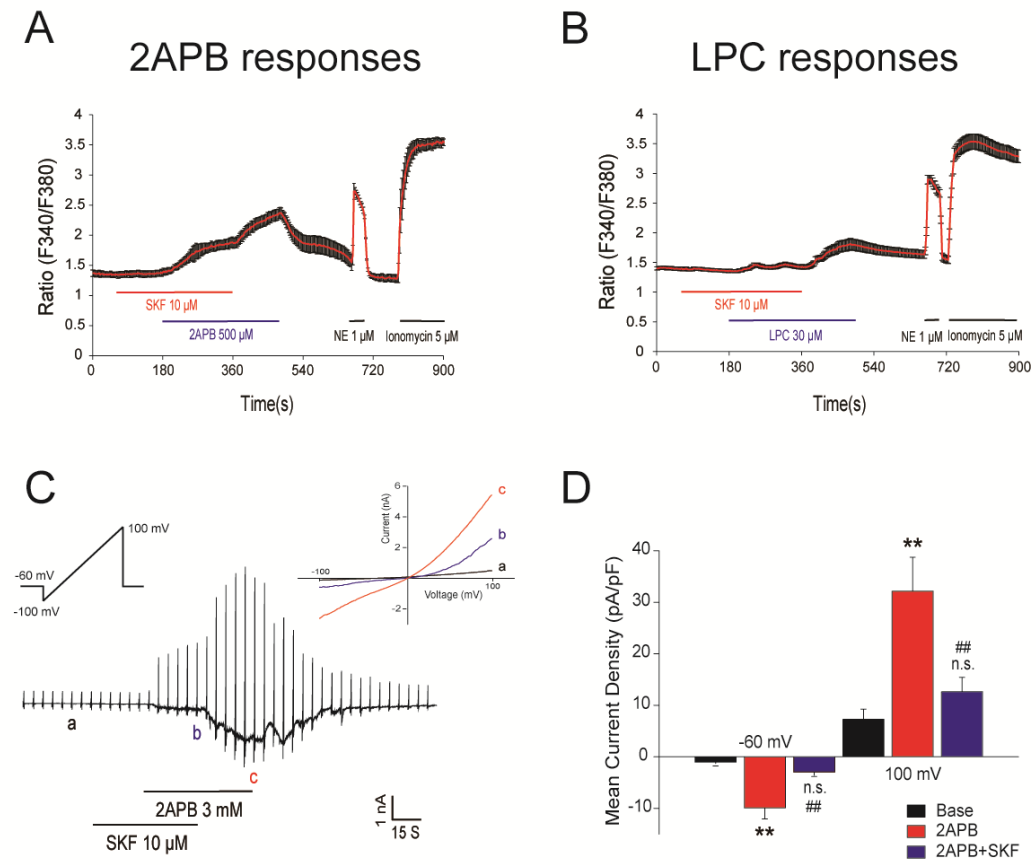
A
2APB responses
Ratio (F340/F380)
SKF 10 μM
2APB 500 μM
NE 1 μM
Ionomycin 5 μM
Time(s)
B
LPC responses
Ratio (F340/F380)
SKF 10 μM
LPC 30 μM
NE 1 μM
Ionomycin 5 μM
Time(s)
C
100 mV
-60 mV
-100 mV
Current (nA)
Voltage (mV)
a
b
c
2APB 3 mM
SKF 10 μM
1 nA
15 S
D
Mean Current Density (pA/pF)
-60 mV
100 mV
n.s.
##
**
Base
2APB
2APB+SKF

Figure 3

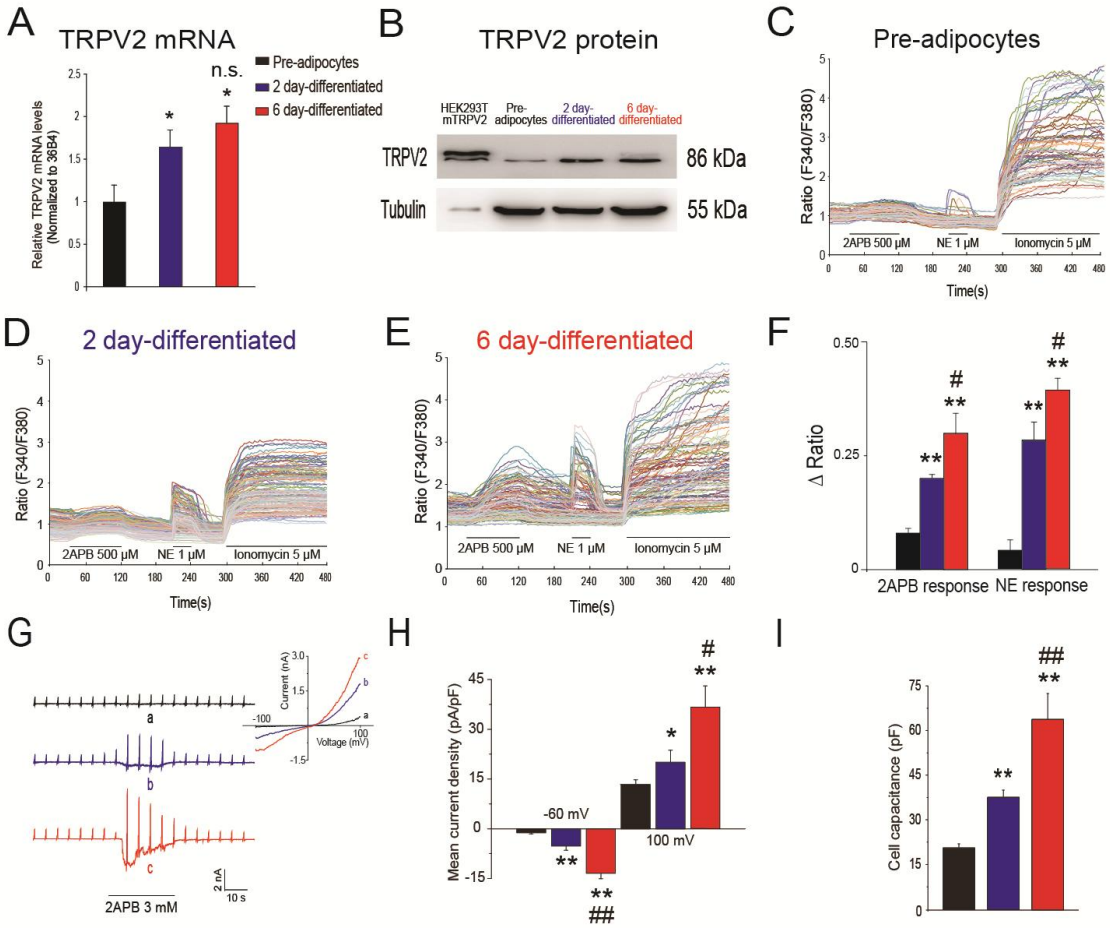
A
TRPV2 mRNA
Pre-adipocytes
2 day-differentiated
6 day-differentiated
n.s.
Relative TRPV2 mRNA levels (Normalized to 36B4)
B
TRPV2 protein
HEK293T mTRPV2
Pre-adipocytes
2 day-differentiated
6 day-differentiated
TRPV2
86 kDa
Tubulin
55 kDa
C
Pre-adipocytes
Ratio (F340/F380)
2APB 500 μM
NE 1 μM
Ionomycin 5 μM
Time(s)
D
2 day-differentiated
E
6 day-differentiated
F
Δ Ratio
2APB response
NE response
G
Current (nA)
Voltage (mV)
2APB 3 mM
H
Mean current density (pA/pF)
-60 mV
100 mV
I
Cell capacitance (pF)

Figure 4

A

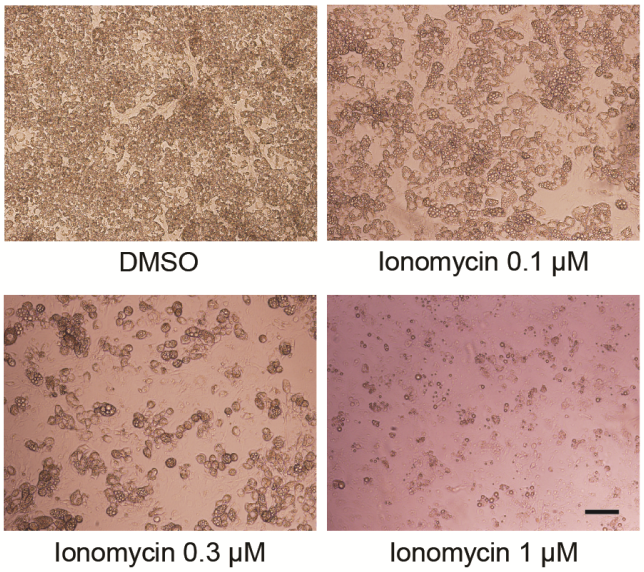
DMSO
Ionomycin 0.1 μM
Ionomycin 0.3 μM
Ionomycin 1 μM

B

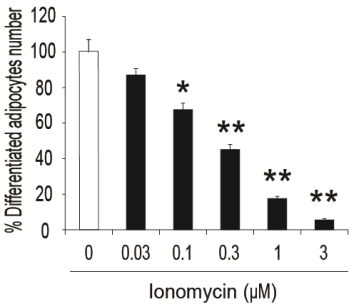
% Differentiated adipocytes number
120
100
80
60
40
20
0
*
**
**
**
0
0.03
0.1
0.3
1
3
Ionomycin (μM)

Figure 5

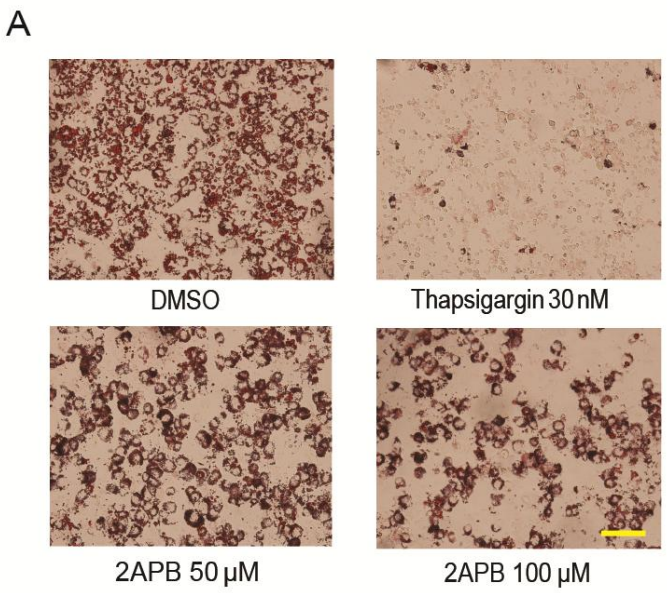
A
DMSO
Thapsigargin 30 nM
2APB 50 µM
2APB 100 µM

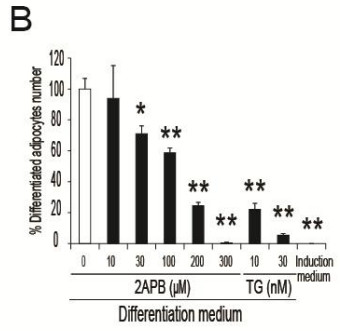
B
% Differentiated adipocytes number
120
100
80
60
40
20
0
0
10
30
100
200
300
10
30
Induction medium
2APB (µM)
TG (nM)
Differentiation medium

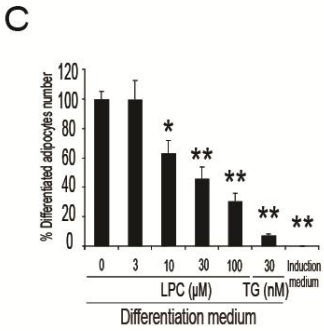
C
% Differentiated adipocytes number
120
100
80
60
40
20
0
0
3
10
30
100
30
Induction medium
LPC (µM)
TG (nM)
Differentiation medium

Figure 6

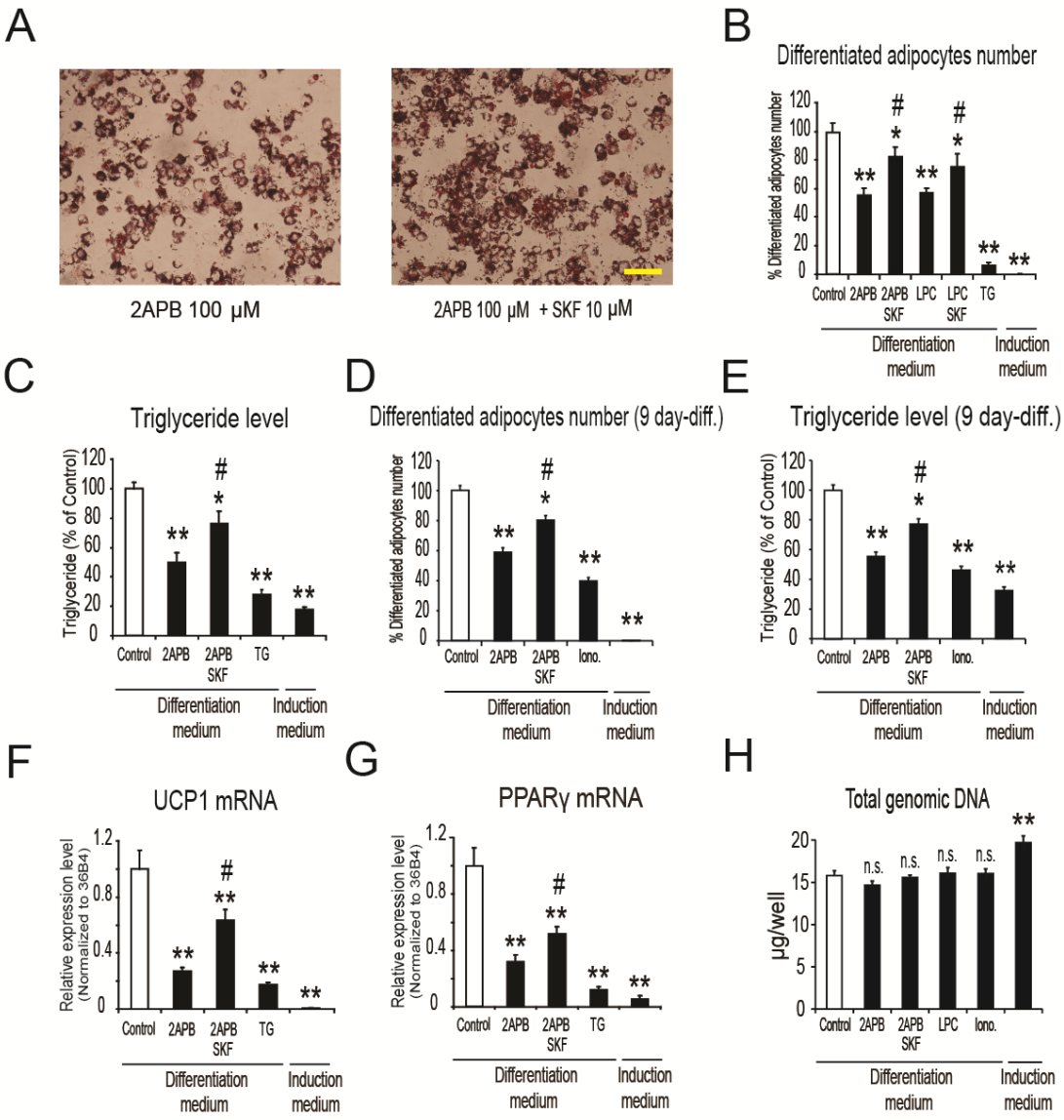
A
2APB 100 μM
2APB 100 μM + SKF 10 μM
B
Differentiated adipocytes number
% Differentiated adipocytes number
Control 2APB 2APB SKF LPC LPC SKF TG
Differentiation medium
Induction medium
C
Triglyceride level
Triglyceride (% of Control)
Control 2APB 2APB SKF TG
Differentiation medium
Induction medium
D
Differentiated adipocytes number (9 day-diff.)
% Differentiated adipocytes number
Control 2APB 2APB SKF Iono.
Differentiation medium
Induction medium
E
Triglyceride level (9 day-diff.)
Triglyceride (% of Control)
Control 2APB 2APB SKF Iono.
Differentiation medium
Induction medium
F
UCP1 mRNA
Relative expression level (Normalized to 36B4)
Control 2APB 2APB SKF TG
Differentiation medium
Induction medium
G
PPARγ mRNA
Relative expression level (Normalized to 36B4)
Control 2APB 2APB SKF TG
Differentiation medium
Induction medium
H
Total genomic DNA
μg/well
n.s.
Control 2APB 2APB SKF LPC Iono.
Differentiation medium
Induction medium

Figure 7

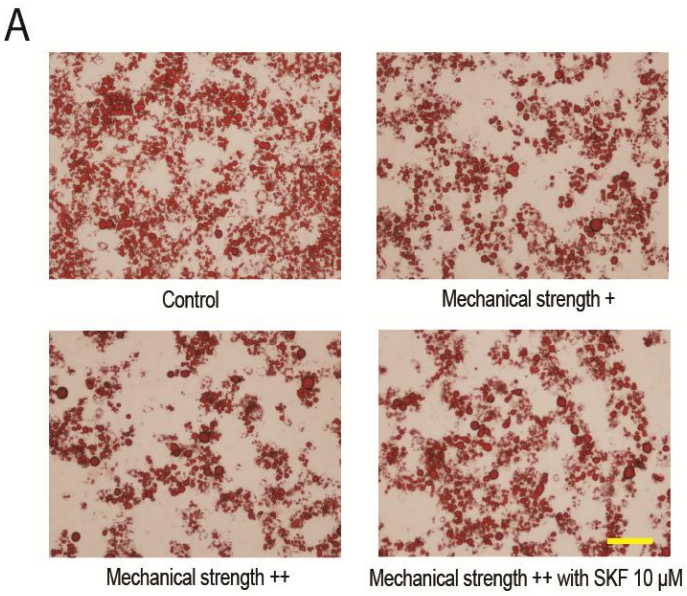
A
Control
Mechanical strength +
Mechanical strength ++
Mechanical strength ++ with SKF 10 µM
B
Differentiated adipocytes number
% Differentiated adipocytes number
120
100
80
60
40
20
0
*
**
#
*
Control
Strength +
Strength ++
Strength ++ SKF 10 µM
Differentiation medium
C
Triglyceride level
Triglyceride (% of Control)
120
100
80
60
40
20
0
*
**
#
*
Control
Strength +
Strength ++
Strength ++ SKF 10 µM
Differentiation medium

Figure 8

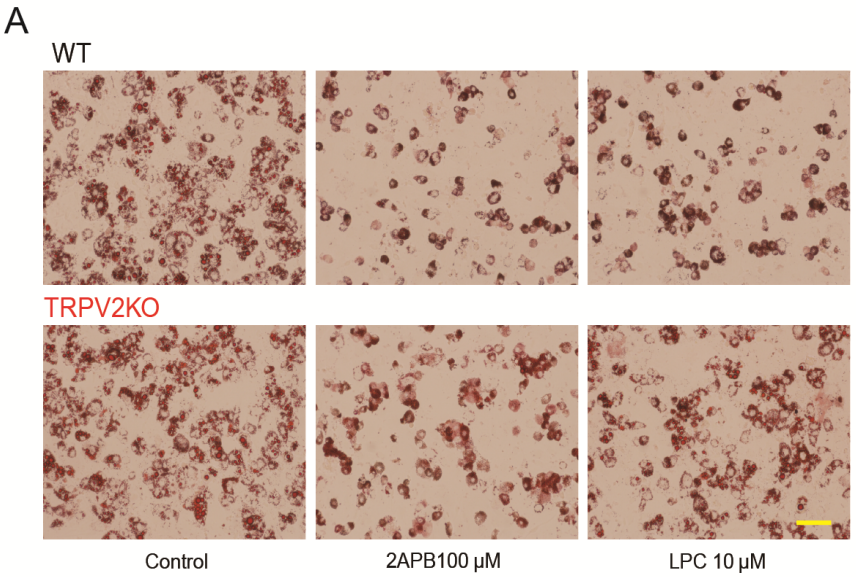
A
WT
TRPV2KO
Control
2APB100 μM
LPC 10 μM

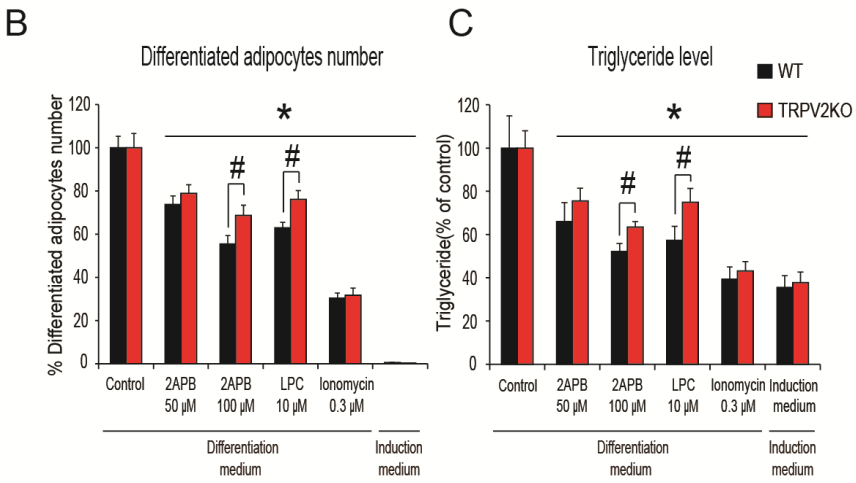
B
Differentiated adipocytes number
% Differentiated adipocytes number
120
100
80
60
40
20
0
*
#
#
Control
2APB 50 μM
2APB 100 μM
LPC 10 μM
Ionomycin 0.3 μM
Differentiation medium
Induction medium
C
Triglyceride level
WT
TRPV2KO
Triglyceride(% of control)
Induction medium

Figure 9

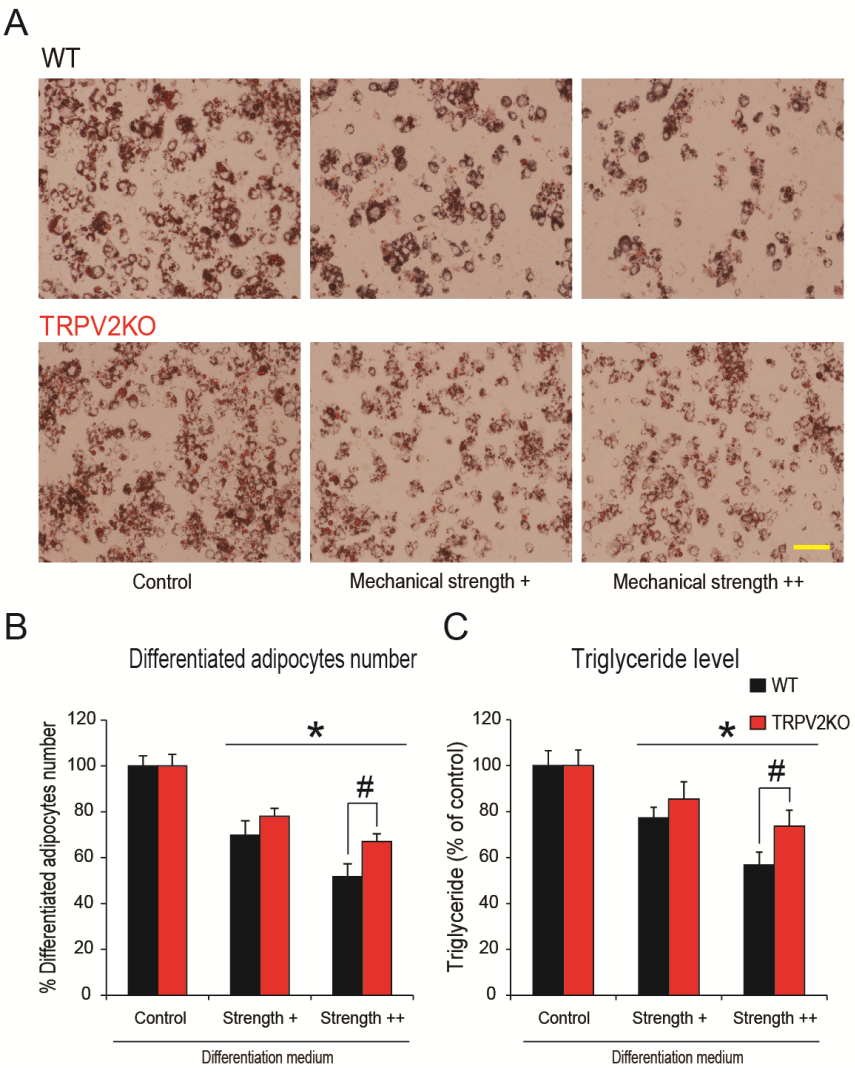
A
WT
TRPV2KO
Control
Mechanical strength +
Mechanical strength ++
B
Differentiated adipocytes number
% Differentiated adipocytes number
120
100
80
60
40
20
0
*
#
Control
Strength +
Strength ++
Differentiation medium
C
Triglyceride level
WT
TRPV2KO
Triglyceride (% of control)
120
100
80
60
40
20
0
*
#
Control
Strength +
Strength ++
Differentiation medium

Figure 10

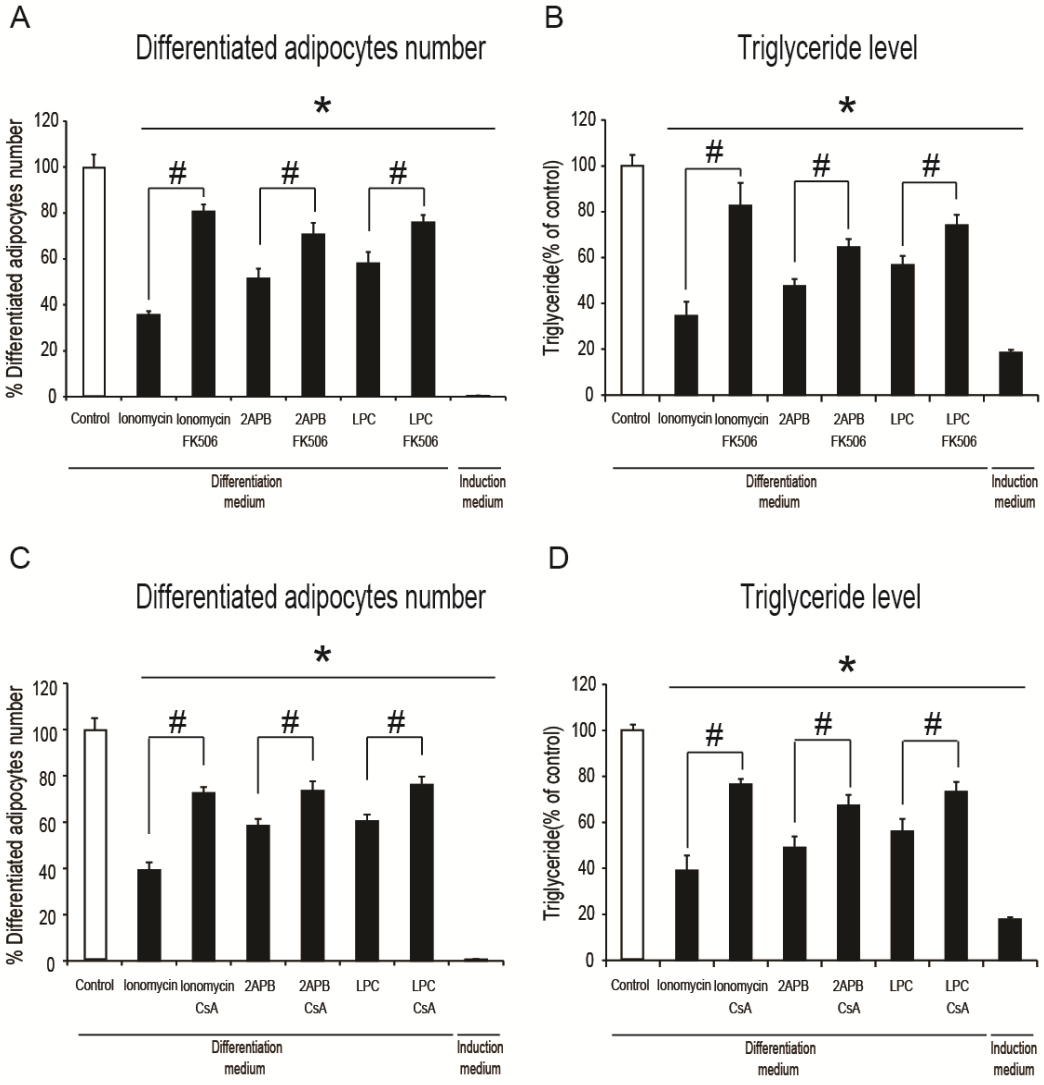
A
Differentiated adipocytes number
% Differentiated adipocytes number
120
100
80
60
40
20
0
*
#
#
#
Control
Ionomycin
Ionomycin FK506
2APB
2APB FK506
LPC
LPC FK506
Differentiation medium
Induction medium
B
Triglyceride level
Triglyceride(% of control)
C
Differentiated adipocytes number
Ionomycin CsA
2APB CsA
LPC CsA
D
Triglyceride level

Figure 11

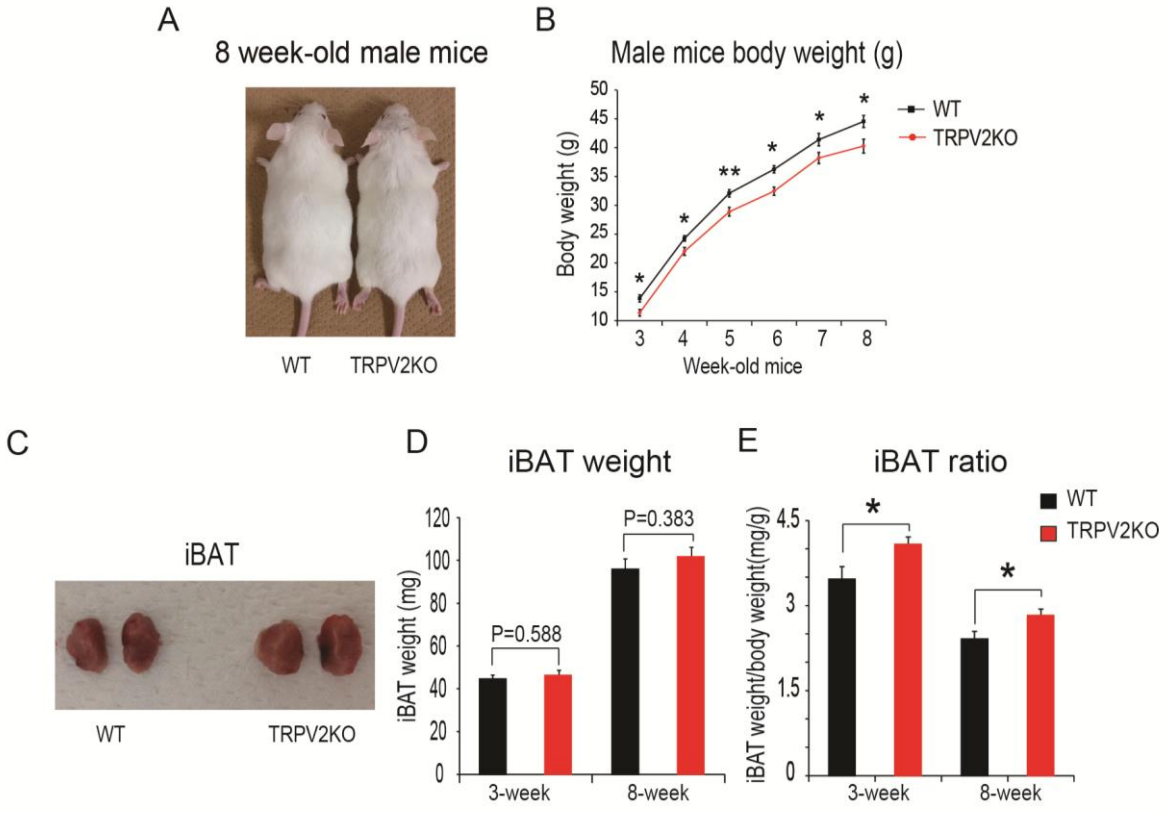
A
8 week-old male mice
WT
TRPV2KO
B
Male mice body weight (g)
Body weight (g)
Week-old mice
WT
TRPV2KO
C
iBAT
WT
TRPV2KO
D
iBAT weight
iBAT weight (mg)
P=0.588
P=0.383
3-week
8-week
E
iBAT ratio
iBAT weight/body weight(mg/g)
WT
TRPV2KO
3-week
8-week

Figure 12

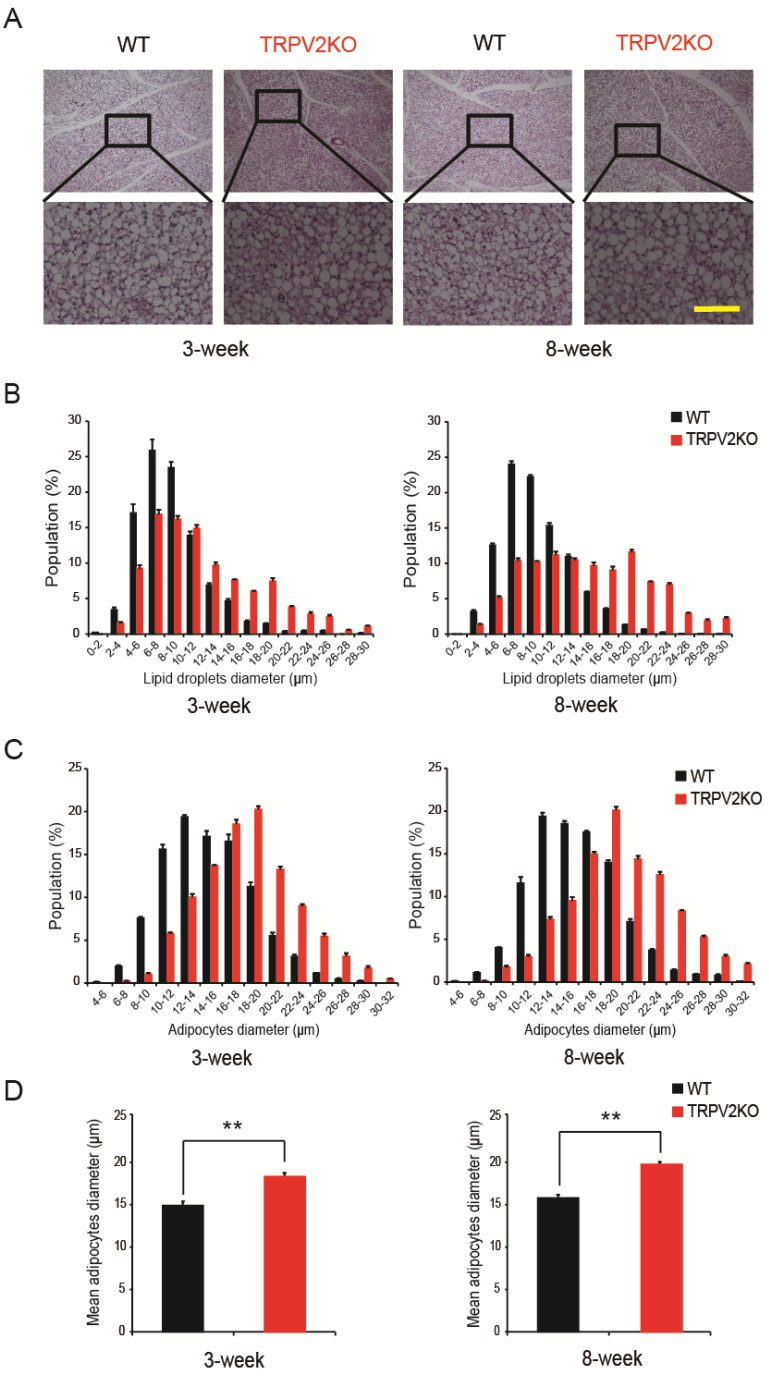
A
WT
TRPV2KO
WT
TRPV2KO
3-week
8-week
B
Population (%)
Lipid droplets diameter (μm)
WT
TRPV2KO
3-week
8-week
C
Population (%)
Adipocytes diameter (μm)
WT
TRPV2KO
3-week
8-week
D
Mean adipocytes diameter (μm)
**
WT
TRPV2KO
3-week
8-week

Figure 13

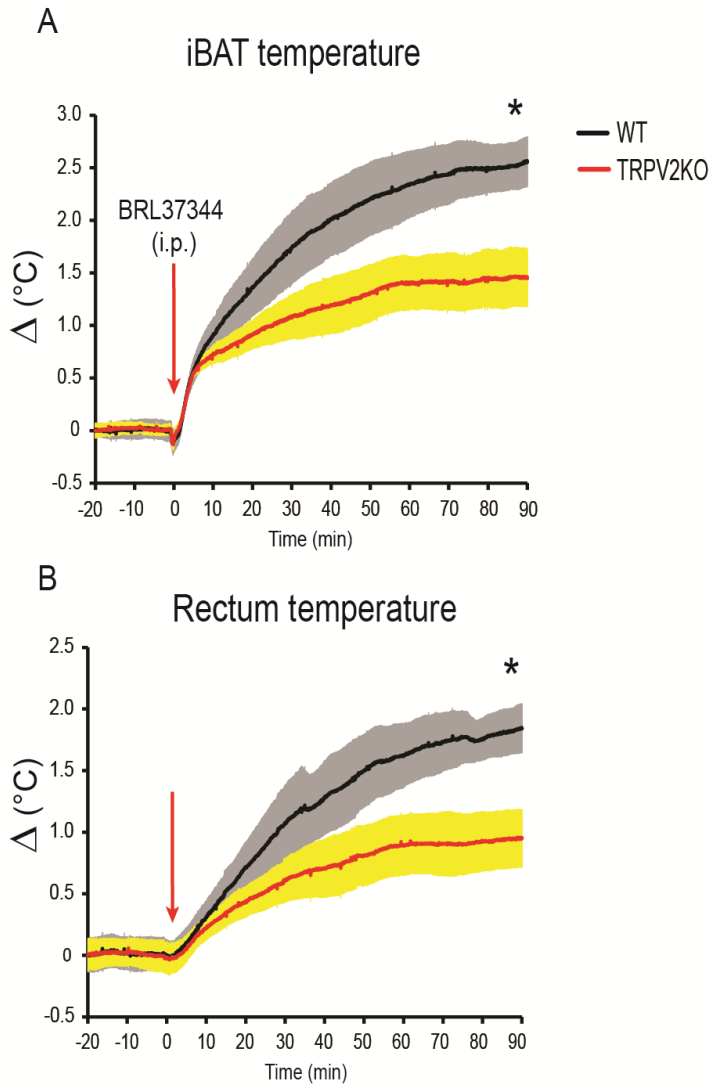
A
iBAT temperature
*
WT
TRPV2KO
BRL37344
(i.p.)
Δ (°C)
3.0
2.5
2.0
1.5
1.0
0.5
0
-0.5
-20 -10 0 10 20 30 40 50 60 70 80 90
Time (min)
B
Rectum temperature
*
Δ (°C)
2.5
2.0
1.5
1.0
0.5
0
-0.5
-20 -10 0 10 20 30 40 50 60 70 80 90
Time (min)

Figure 14

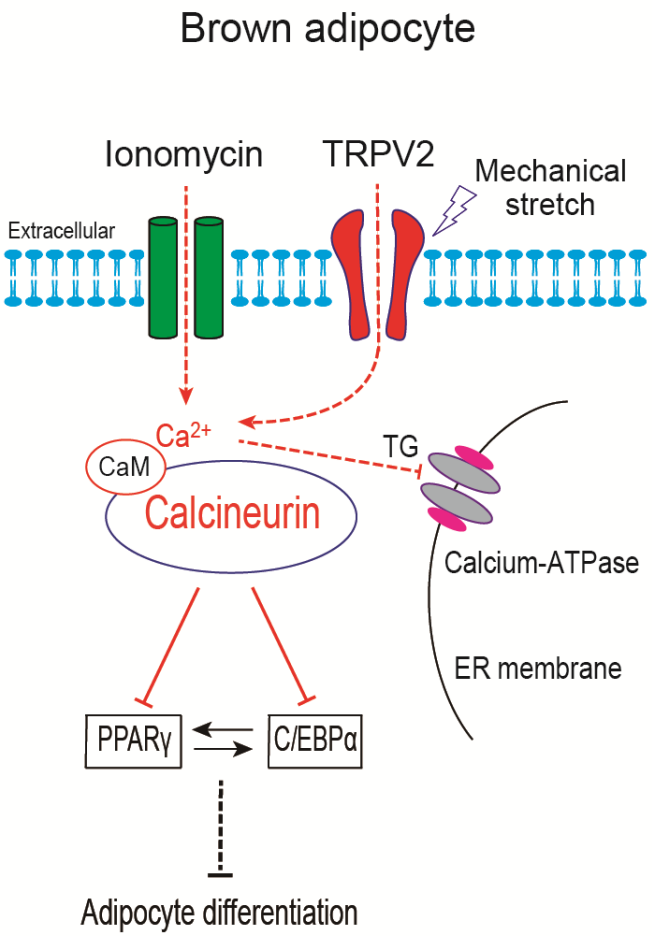
Brown adipocyte
Ionomycin
TRPV2
Mechanical stretch
Extracellular
Ca2+
CaM
Calcineurin
TG
Calcium-ATPase
ER membrane
PPARγ
C/EBPα
Adipocyte differentiation

8. Abbreviations

AA	amino acids
2-APB	2-aminoethoxydiphenyl borate
bp	base pair
g	gram
IP	immunoprecipitation
kDa	kilodalton
ms	milli second
mV	milli volt
mRNA	messenger ribonucleic acid
mTRPV2	mouse transient receptor potential vanilloid 2
µM	micro molar
µm	micro meter
N	number
nA	nano ampere
n.s.	no significant differences
pA	pico ampere
pF	pico farad
Realtime RT-PCR	realtime reverse transcription-polymerase chain reaction
RT-PCR	reverse transcription-polymerase chain reaction
s	second
SDS-PAGE	sodium dodecyl sulfate-polyacrylamide gel electrophoresis

TM	transmembrane domain
TRPV	transient receptor potential vanilloid
TRPA1KO	transient receptor potential vanilloid 2 knock-out
BSA	bovine serum albumin
CaM	calmodulin
C/EBP-α	CCAAT/enhancer-binding protein-alpha
CsA	cyclosporin A
Ct.	control
DM	differentiation Medium
DMEM	dulbecco's modified Eagle's medium
Dex	dexamethasone
ER	endoplasmic reticulum
FBS	fetal bovine serum
IBMX	3-isobutyl-1-methylxanthine
PBS	phosphate buffered saline
UCP1	uncoupling protein 1
PPAR-γ	peroxidase proliferator-activated regulator-gamma
PVDF	polyvinylidene difluoride
RIPA	radioimminoprecipitation assay buffer
TG	thapsigargin
T3	triiodothyronine
WT	wild type
WAT	white adipose tissue

BAT	brown adipose tissue
iBAT	interscapular brown adipose tissue
Iono.	ionomycin
3T3-L1	cell line which was originated from clonal expansion of murine Swiss 3T3 cells and contain only a single cell type
LPC	lysophosphatidyl choline
SKF	SKF96365
NE	norepinephrine
i.p.	intraperitoneal

9. Acknowledgements

I sincerely acknowledge and express my heartfelt thanks to my supervisor, Professor Makoto Tominaga for giving me such a great chance to work in his laboratory. And I would like to thank him for his great support and guidance throughout my study in NIPS, Japan. Also, I would like to appreciate the help and advice provided by my advisory committee, Assistant Professor Kunitoshi Uchida and Assistant Professor Yoshiro Suzuki. As well, I want to express my many thanks to Dr. Yiming Zhou and Dr. Yasunori Takayama for their technical support and discussion. And also I would like to appreciate all of my lab members for their kind help not only in my study but also in my life in Japan throughout my study.

Moreover, I really very much appreciate my collaborators, Professor Teruo Kawada and Assistant Professor Nobuyuki Takahashi in Kyoto University for their kind discussion, and Assistant Professor Tsuyoshi Goto and Dr. Minji Kim for their teaching me adipocyte primary culture technique.

In addition, I would like to thank, Director Shigeo Wakabayashi and Laboratory chief Yuko Iwata in National Cerebral and Cardiovascular Center of Japan for their generously providing TRPV2KO mice to me.

I also thank the many people around me both in and out of the lab for their help and support.

Finally, I would like to thank my parents, my wife, and my brother for their continuous support and encouragement far away from China. And I thank to my wife for forgiving and understanding me.